Electronic Supplementary Material (ESI) for RSC Advances.

Supplementary Information

Phomeketales A-F, six unique metabolites from the endophytic fungus *Phoma* sp.YN02-P-3

Xia-Nan Sang,[ab] Shao-Fei Chen,[ab] Gang Chen,[ab] Xiao An,[ab] Sheng-Ge Li,[ab] Xiao-Ni Li,[ab] Bin Lin,[cd] Jiao Bai,[ab] Hai-Feng Wang*[ab] and Yue-Hu Pei*[ab]

[a]*Key Laboratory of Structure-Based Drug Design & Discovery, Ministry of Education, Shenyang Pharmaceutical University, Shenyang 110016, China.*

[b]*School of Traditional Chinese Materia Medica, Shenyang Pharmaceutical University, Shenyang 110016, China.*

[c]*Department of Medicinal Chemistry, School of Pharmaceutical Engineering, Shenyang Pharmaceutical University, Shenyang 110016, People's Republic of China*

[d]*Key Laboratory of Structure-Based Drug Design & Discovery, Ministry of Education, Shenyang Pharmaceutical University, Shenyang 110016, People's Republic of China*

Contents

1. General experimental procedures ·····6

2. Fungal material and fermentation ·····6

3. Extraction and isolation ·····7

Physicochemical data·····8

4. Bioassays ·····9

(1) *Cytotoxic assay* ·····9

(2) *Anti-AChE activity assay* ·····10

5. The spectra of Phomeketale A (**1**) ·····11

Figure S1. The UV spectrum of compound **1** ·····11

Figure S2. The IR spectrum of compound **1** ·····11

Figure S3. The HR-ESI-MS spectrum of compound **1** ·····12

Figure S4. The ^{1}H-NMR spectrum of compound **1** ·····12

Figure S5. The ^{13}C-NMR spectrum of compound **1** ·····13

Figure S6. The HSQC spectrum of compound **1** ·····13

Figure S7. The HMBC spectrum of compound **1** ·····14

Figure S8. The NOESY spectrum of compound **1** ·····14

Computational details for ECD of compound **1** ·····15

Figure S9. B3LYP/6-31 G* optimized lowest energy 3D conformer of **1** ·····18

Figure S10. Experimental and suitable calculated ECD spectra of **1** ·····18

6. The spectra of Phomeketale B (**2**) ·····19

Figure S11. The UV spectrum of compound **2** ·····19

Figure S12. The IR spectrum of compound **2** ·····19

Figure S13. The HR-ESI-MS spectrum of compound **2** ·····20

Figure S14. The ^{1}H-NMR spectrum of compound **2** ·····20

Figure S15. The ^{13}C-NMR spectrum of compound **2** ·····21

Figure S16. The HSQC spectrum of compound **2** ·····21

Figure S17. The HMBC spectrum of compound **2** ·····22

Figure S18. The NOESY spectrum of compound **2** ·····23

Computational details for ECD of compound **2** ·····24

Figure S19. B3LYP/6-31 G* optimized lowest energy 3D conformer of **2** ·····26

Figure S20. Experimental and suitable calculated ECD spectra of **2** ·····26

7. The spectra of Phomeketale C (**3**) ·····27

Figure S21. The UV spectrum of compound **3** ·····27

Figure S22. The IR spectrum of compound **3** ·····27

Figure S23. The HR-ESI-MS spectrum of compound **3** ·····28

Figure S24. The ^{1}H-NMR spectrum of compound **3** ·····28

Figure S25. The ^{13}C-NMR spectrum of compound **3** ·····29

Figure S26. The HMQC spectrum of compound **3** ·····29

Figure S27. The HMBC spectrum of compound **3** ·····30

Figure S28. The NOESY spectrum of compound **3** ·····30

Computational details for ECD of compound **3** ·····31

Figure S29. B3LYP/6-31 G* optimized lowest energy 3D conformer of **3** ·····33

Figure S30. Experimental and suitable calculated ECD spectra of **3** ·····34

8. The spectra of Phomeketale D (**4**) ·····34

Figure S31. The UV spectrum of compound **4** ·····34

Figure S32. The IR spectrum of compound **4** ·····35

Figure S33. The HR-ESI-MS spectrum of compound **4** ·····35

Figure S34. The ^{1}H-NMR spectrum of compound **4** ·····36

Figure S35. The ^{13}C-NMR spectrum of compound **4** ·····36

Figure S36. The HSQC spectrum of compound **4** ·····37

Figure S37. The HMBC spectrum of compound **4** ·····37

Figure S38. The NOESY spectrum of compound **4** ·····38

Computational details for ECD of compound **4** ·····38

Figure S39. B3LYP/6-31 G* optimized lowest energy 3D conformer of **4** ·····41

Figure S40. Experimental and suitable calculated ECD spectra of **4** ·····41

Figure S41. The CD spectrum of compound **4** in a $CDCl_3$ of $[Rh_2(OCOCF_3)_4]$ (the inherent contribution of compound **4** was subtracted) ·····42

9. The spectra of Phomeketale E (**5**)·····42

Figure S42. The UV spectrum of compound **5** ·····42

Figure S43. The IR spectrum of compound **5**·····43

Figure S44. The HR-ESI-MS spectrum of compound **5**·····43

Figure S45. The ^{1}H-NMR spectrum of compound **5** ·····44

Figure S46. The ^{13}C-NMR spectrum of compound **5** ·····44

Figure S47. The HSQC spectrum of compound **5** ·····45

Figure S48. The HMBC spectrum of compound **5**·····45

Figure S49. The NOESY spectrum of compound **5** ·····46

Computational details for ECD of compound **5** ·····47

Figure S50. B3LYP/6-31 G* optimized lowest energy 3D conformer of **5** ·····50

Figure S51. Experimental and suitable calculated ECD spectra of **5** ·····50

10. The spectra of Phomeketale F (**6**)·····50

Figure S52. The UV spectrum of compound **6** ·····51

Figure S53. The IR spectrum of compound **6**·····51

Figure S54. The HR-ESI-MS spectrum of compound **6**·····52

Figure S55. The ^{1}H-NMR spectrum of compound **6** ·····52

Figure S56. The ^{13}C-NMR spectrum of compound **6** ·····53

Figure S57. The HSQC spectrum of compound **6** ·····53

Figure S58. The HMBC spectrum of compound **6** ·····54

Figure S59. The NOESY spectrum of compound **6** ·····54

Computational details for ECD of compound **6** ·····56

Figure S60. B3LYP/6-31 G* optimized lowest energy 3D conformer of **6** ·····61

Figure S61. Experimental and suitable calculated ECD spectra of **6** ·····62

1. General experimental procedures

Optical rotation was measured with a JASCO P-2000 Series (Jasco Co., Ltd, Tokyo, Japan). The UV spectrum was recorded on a Shimadzu UV-2201 spectrophotometer (Shimadzu Corporation, Kyoto, Japan). The IR spectrum was obtained from a Bruker IFS-55 spectrophotometer using KBr pellet (Bruker Optik BmbH, Ettlingen, Germany). The HR-ESI-MS data were obtained on a microTOF-Q Bruker mass instrument (Bruker Daltonics, Billerica, MA, USA). CD spectra were recorded with a Biologic MOS-450 spectrometer using $CDCl_3$ as solvent. 1D and 2D NMR spectra were run on a Bruker AVANCE-400/-600 spectrometer (Bruker BioSpin GmbH, Rheinstetten, Germany). ^1H chemical shifts (δ_H) were measured in ppm, relative to TMS, and ^{13}C chemical shifts (δ_C) were measured relative to DMSO-d_6 and converted to TMS scale. Column chromatography (CC) was performed on Silica gel (200–300 mesh; Qingdao Marine Chemical Co., Qingdao, China) and Sephadex LH-20 (Pharmacia, Uppsala, Sweden) columns. Analytical and preparative thin-layer chromatographies (TLC) were carried out using silica gel plates (GF254 10-40 μm，Qingdao Marine Chemical Co., China). Analytical TLC was used to follow the separation and check the purity of isolated compounds. Spots on the plates were observed under UV light and visualized by spraying 10% H_2SO_4 in EtOH (v/v), followed by heating. HPLC was performed on a Shimadzu LC-10AVP liquid chromatograph with a YMC-pack C_{18} (ODS) column (10 × 250 mm, 5 μm, Japan) and a Shimadzu LC-8AVP liquid chromatograph with a Diamonsil C_{18} (ODS) column (4.6 × 250 mm, 5 μm, China). All reagents were HPLC or analytical grade and were purchased from Tianjin Damao Chemical Company (Tianjin, China).

2. Fungal material and fermentation

The fungal strain YN02-P-3 was isolated from the plant *Sumbaviopsis* J. J. Smith in Yunnan, P.R. China in September 2013. It was identified as *Phoma* sp. YN02-P-3 (GenBank accession no. KU522468) and has been deposited in the School of Traditional Chinese Materia Medica, Shenyang Pharmaceutical University.

The fungal strain YN02-P-3 was cultured on slants of potato dextrose agar at 25 °C for 10 days. Agar plugs were inoculated in 500 mL Erlenmeyer flask containing 120 mL of

media (0.4% glucose,1% malt extract, and 0.4% yeast extract; the final pH of the media was adjusted to 6.5) before sterilization, and incubated at 25 °C on a rotary shaker at 170 rpm for one week. Large scale fermentation was carried out in one hundred and fifty 500 mL Fernbach flasks each containing 80 g of rice and 120 mL of distilled H_2O. Each flask was inoculated with 5.0 mL of the culture medium and incubated at 25 °C for 40 days.

3. Extraction and isolation

The solid culture of *Phoma* sp. YN02-P-3 on cooked rice was extracted with 95% EtOH (1×150 mL) under ultrasonic 2 times, and 85% EtOH (1×150 mL), each time for twenty minutes, respectively. The combined extracts were concentrated in vacuo to yield a residue, which was suspended in H_2O, successively partitioned with ethyl acetate and *n*-butanol. The EtOAc crude extracts (50.0 g) were applied on a silica gel column and eluted with Petroleum-Acetone gradient (from 100:0 to 0:100) to afford 9 fractions. Fr. 2 purified by semi-preparative HPLC on ODS column eluted with 57% MeOH-H_2O to yield compound **2** (15 mg), Fr. 4 using silica gel column chromatography eluting with Petroleum-ethyl acetate (from 100:0 to 0:100) to give 3 subfractions. Fr.4-1 purified by semi-preparative HPLC on ODS column eluted with 60% MeOH-H_2O to yield compound **6** (19 mg), Fr.4-2 (7 g) was further subjected to MPLC on ODS with MeOH-H_2O (20:80, 40:60, 60:40, 80:20 and 100:0, v/v) and purified by semi-preparative HPLC on ODS column eluted with 45% MeOH-H_2O (Fr. 5) to yield compound **5** (35 mg), Fr. 5 using silica gel column chromatography eluting with Petroleum-ethyl acetate (from 100:0 to 0:100) to give 5 subfractions. Fr.5-2 was further purified using silica gel column chromatography eluting with Petroleum-Acetone (from 100:0 to 0:100) to give 9 subfractions. Fr.5-2-4 and Fr.5-2-4 were further subjected to MPLC on ODS with MeOH-H_2O (20:80, 40:60, 60:40, 80:20 and 100:0, v/v) and purified by semi-preparative HPLC on ODS column eluted with 40% MeOH-H_2O (Fr.5-2-4) to yield compound **1** (8 mg), with 55% MeOH-H_2O (Fr.5-2-4) to yield compound **4** (4.2 mg), and with 65% MeOH-H_2O (Fr.5-2-4) to yield compound **3** (7 mg).

Physicochemical data

Phomeketale A (**1**): a yellow oil (MeOH); $[\alpha]_D^{20}$ (*c* 0.40, MeOH) +7.25; UV (MeOH) $\lambda_{max}(\log\varepsilon)$: 207 (4.12), 286 (3.21) nm; IR (KBr) ν_{max}: 3429, 1638, 1383cm^{-1}; ^{13}C and ^{1}H NMR data, see Table 1; CD (MeOH) λ_{max} ($\Delta\varepsilon$) : 204 (+1.0), 234 (−11.6), 285 (+5.0) nm; (+)-HRESIMS *m/z* 315.1216 $[M+Na]^+$ (calcd for $C_{16}H_{20}Na_1O_5$, 315.1203);

Phomeketale B (**2**): a yellow amphorous powder (MeOH); $[\alpha]_D^{20}$ (*c* 0.40, MeOH) -22.25; UV (MeOH) $\lambda_{max}(\log\varepsilon)$: 209 (4.06), 233 (3.93), 279 (3.91), 320 (3.6)nm; IR (KBr) ν_{max}: 3424, 1667, 1322 cm^{-1}; CD (MeOH) λ_{max} ($\Delta\varepsilon$) : 204 (−7.8), 238 (+2.5), 279 (−5.2) nm; ^{13}C and ^{1}H NMR data, see Table 1; (+)-HRESIMS *m/z* 299.1252 $[M+Na]^+$ (calcd for $C_{16}H_{20}Na_1O_4$, 299.1254);

Phomeketale C (**3**): a yellow amphorous powder; $[\alpha]_D^{20}$ (*c* 0.50, MeOH) −2.87; UV (MeOH) λ_{max} ($\log\varepsilon$): 208 (4.79), 284 (4.16), 319 (4.05) nm; IR (KBr) ν_{max}: 3427, 1632, 1383cm^{-1}; CD (MeOH) λ_{max} ($\Delta\varepsilon$) : 202 (+12.9), 216 (+1.3), 221 (+24.0), 232 (−59.7) nm; ^{13}C and ^{1}H NMR data, see Table 2; (+)-HRESIMS *m/z* 449.1554 $[M-H2O+Na]^+$ (calcd for $C_{24}H_{26}Na_1O_7$, 465.2272);

Phomeketale D (**4**): a yellow oil; $[\alpha]_D^{20}$ (*c* 0.40, MeOH) -9.45; UV (MeOH) λ_{max} ($\log\varepsilon$): 207 (3.62), 265 (4.17) nm; IR (KBr) ν_{max}: 3429, 1637, 1384cm^{-1}; CD ($CDCl_3$) λ_{max} ($\Delta\varepsilon$) : 202 (+5.1), 212 (−9.2), 225 (+17.7), 264 (−28.9) nm; ^{13}C and ^{1}H NMR data, see Table 3; (+)-HRESIMS *m/z* 385.1628 $[M+Na]^+$ (calcd for $C_{20}H_{26}Na_1O_6$, 385.1622);

Phomeketale E (**5**): a white needles; $[\alpha]_D^{20}$ (*c* 0.78, MeOH) -44.80; UV (MeOH) λ_{max} ($\log\varepsilon$): 208 (4.22), 252 (3.54), 316 (3.48) nm; IR (KBr) ν_{max}: 3432, 1630, 1384, 1119cm^{-1}; CD (MeOH) λ_{max} ($\Delta\varepsilon$) : 199 (+10.5), 231 (−13.4), 245 (+11.0), 264 (−28.1) nm; ^{13}C and ^{1}H NMR data, see Table 3; (+)-HRESIMS *m/z* 299.0918 $[M-H_2O+Na]^+$ (calcd for $C_{24}H_{26}Na_1O_7$, 299.0918);

Phomeketale F (**6**): a white needles; $[\alpha]_D^{20}$ (*c* 0.65, MeOH) -32.55; UV (MeOH) λ_{max} ($\log\varepsilon$): 214 (4.30), 258 (3.65), 312 (3.43) nm; IR (KBr) ν_{max}: 3428, 1756, 1619, 1345,

1117cm^{-1}; CD (MeOH) λ_{max} ($\Delta\varepsilon$) : 214 (−3.7), 224 (+7.4), 235 (−13.9), 249 (+6.6), 268 (−20.8) nm; ^{13}C and ^{1}H NMR data, see Table 2; (+)-HRESIMS *m/z* 409.1623 [M-H_2O+Na]$^+$ (calcd for $C_{22}H_{26}Na_1O_6$, 409.1622);

4. Bioassays

(1) *Cytotoxic assay*

Cytotoxic activities of isolated compounds **1**-**6** and the positive control 5-fluorouracil were evaluated by the trypan blue method[1, 2] against the human leukaemia cell lines (HL-60) and the human acute myeloid leukemia cell lines (Molm 13), and the MTT assay[3] using the prostate cancer cell lines (PC-3). The cell lines were purchased from America Type Culture Collection, ATCC (Rockville, MD, USA) and cultured in RPMI-1640 medium (Gibco, New York, NY, USA) supplemented with 100 U/mL penicillin, 100 μg/mL streptomycin, 1 mM glutamine and 10% heat-inactivated foetal bovine serum (Gibco) at 37 °C in humidified atmosphere with 5% CO_2.

The human leukaemia cell lines (HL-60) and the human acute myeloid leukemia cell lines (Molm 13) (American Type Culture Collection, Rockville, MD, USA) were cultured in the above medium at a density of 5×10^4 cells/mL at 37 under an atmosphere of 5% CO_2. Cell growth inhibition assay was performed as reported previously. The compounds were dissolved in DMSO, and the amount of DMSO was controlled lower than 0.1% in the final concentration. Cells were incubated with various drug concentrations for 3 days. The number of cells was determined by hemocytometer, and its viability was determined using trypan blue staining. The growth inhibitory ability of the compound was calculated and expressed using the IC_{50} value (half-inhibitory concentration). 5-Fluorouracil (5-FU) and 0.1% DMSO were used as a positive control and a negative control, respectively.

In the MTT assay, briefly, cells suspensions, 200 μl, at a density of 2.5×104 cells/mL, were plated in 96-well microtiter plates and incubated for 24 h at 37 °C under 5% CO_2 and 95% air. Then the test compounds with different concentrations in DMSO were placed into each microtiter plates and further incubated for 72 h. Finally, 50 μl of a 0.4% MTT solution was added to each well and incubated for 4 h. Then, the MTT was

removed from the wells and the fromazan crystals were dissolved in DMSO (200 μl) for 10 min with shaking. Then the plate was read immediately on a microtiter plate reader (Bio-RAD) at a wavelength of 570 nm to record the optical density (OD). The IC_{50} value was defined as the concentration of the control in the MTT assay. 5-Fluorouracil (5-Fu) was used as a positive control.

(2) *Anti-AChE activity assay*

A mix of 25μl DTNB [5, 5'-dithio-bis (2-nitrobenzoic acid)] (4.0mM) and 25μl enzyme solution (0.01U/ml) was incubated at 37 °C in 96-well plates in the presence of 25-compounds (50μl). The reaction was started by adding 25μl substrat solution (butyrylcholine chlride, 0.4mM) and incubated for 40min. Then, the absorbance of reaction product was tested at 405nm (Bio-Rad Model 680 Automatic microplate reader, Thrmo Fischer Scientific oy, Finland) [4].

$$\text{Inhibitory rate}\,(\%) = 100 * \frac{A_{405}(\text{enzyme}) - A_{405}(\text{compound})}{A_{405}(\text{enzyme}) - A_{405}(\text{blank})}$$

References:

[1] F. Wang, H. M. Hua, Y. H. Pei, D. Chen, and Y. K. Jing, *J. Nat. Prod.*, 2006, **69**, 807-810.

[2] J. Hu, X. D. Shi, J. G. Chen, X. Mao, L. Zhu, L. YU, and J. Y. Shi, *Food Chem*., 2014, **148**, 437–444.

[3] K. B. Wang, Y. T. Di, Y. Bao, C.M. Yuan, G. Chen, D. H. Li, J. Bai, H. P. He, X. J. Hao, Y. H. Pei, Y. K. Jing, Z. L. Li, and H. M. Hua, *Org. Lett*., 2014, **16**, 4028−4031.

[5] R. León, C. Ríos, M.C. José, H. Oscar, B. Xavier, F.J. Luque, M.G. Lépez, A.G. Garcíab and M. Villarroya, *Bioorg. Med. Chem*. 2008, **16**, 7759

5. The spectra of Phomeketale A (1)

Figure S1. The UV spectrum of compound **1**

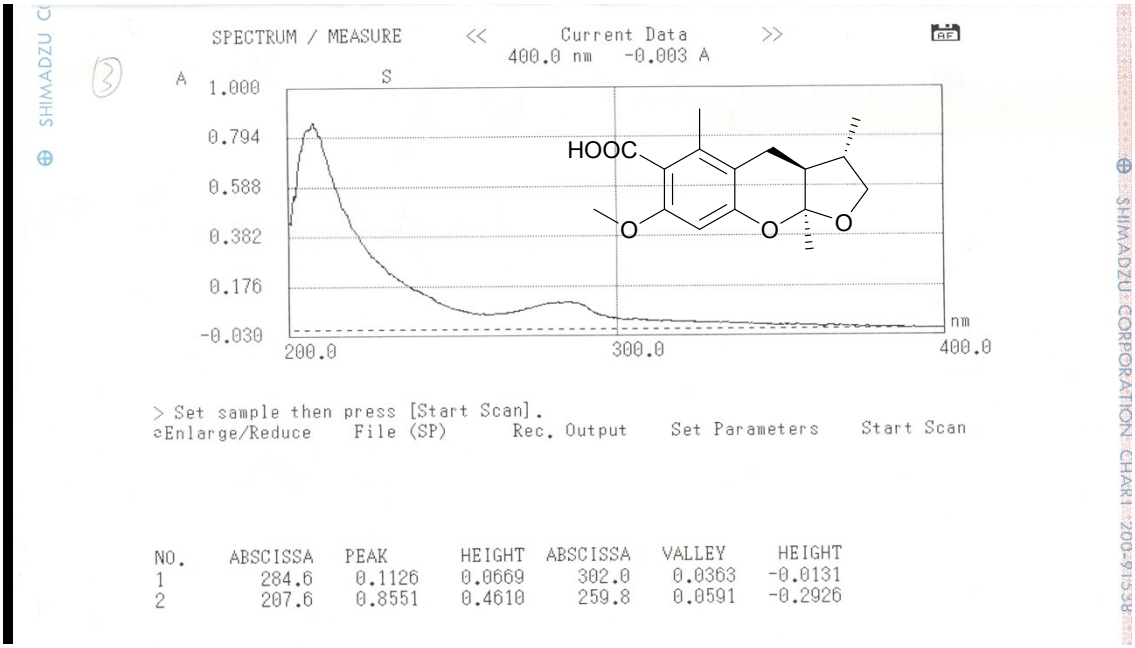

Figure S2. The IR spectrum of compound **1**

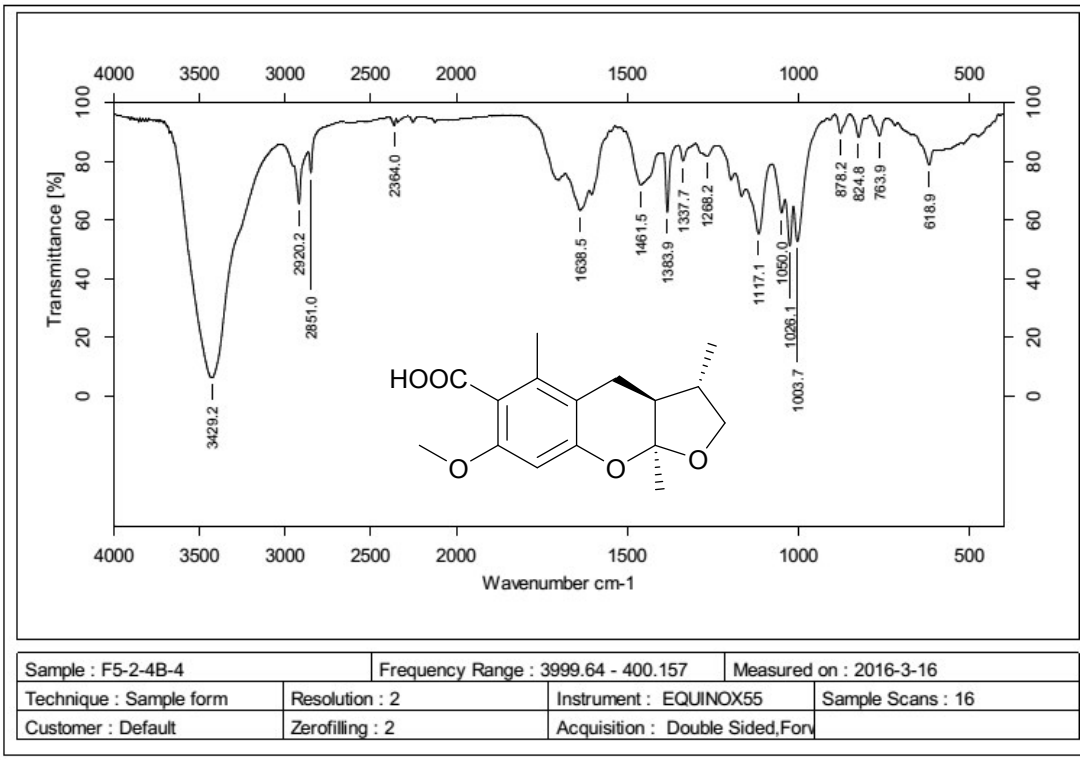

Figure S3. The HR-ESI-MS spectrum of compound **1**

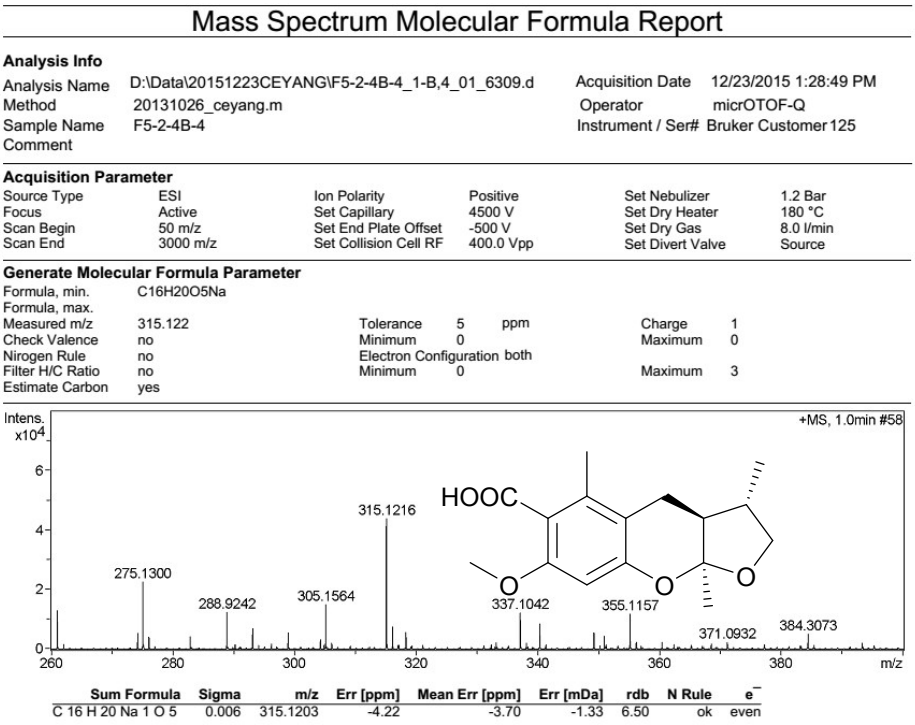

Mass Spectrum Molecular Formula Report

Analysis Info

Analysis Name	D:\Data\20151223CEYANG\F5-2-4B-4_1-B,4_01_6309.d	Acquisition Date	12/23/2015 1:28:49 PM
Method	20131026_ceyang.m	Operator	micrOTOF-Q
Sample Name	F5-2-4B-4	Instrument / Ser#	Bruker Customer 125
Comment			

Acquisition Parameter

Source Type	ESI	Ion Polarity	Positive	Set Nebulizer	1.2 Bar
Focus	Active	Set Capillary	4500 V	Set Dry Heater	180 °C
Scan Begin	50 m/z	Set End Plate Offset	-500 V	Set Dry Gas	8.0 l/min
Scan End	3000 m/z	Set Collision Cell RF	400.0 Vpp	Set Divert Valve	Source

Generate Molecular Formula Parameter

Formula, min.	C16H20O5Na						
Formula, max.							
Measured m/z	315.122	Tolerance	5	ppm	Charge	1	
Check Valence	no	Minimum	0		Maximum	0	
Nirogen Rule	no	Electron Configuration	both				
Filter H/C Ratio	no	Minimum	0		Maximum	3	
Estimate Carbon	yes						

Sum Formula	Sigma	m/z	Err [ppm]	Mean Err [ppm]	Err [mDa]	rdb	N Rule	e⁻
C 16 H 20 Na 1 O 5	0.006	315.1203	-4.22	-3.70	-1.33	6.50	ok	even

Figure S4. The ^{1}H-NMR spectrum of compound **1**

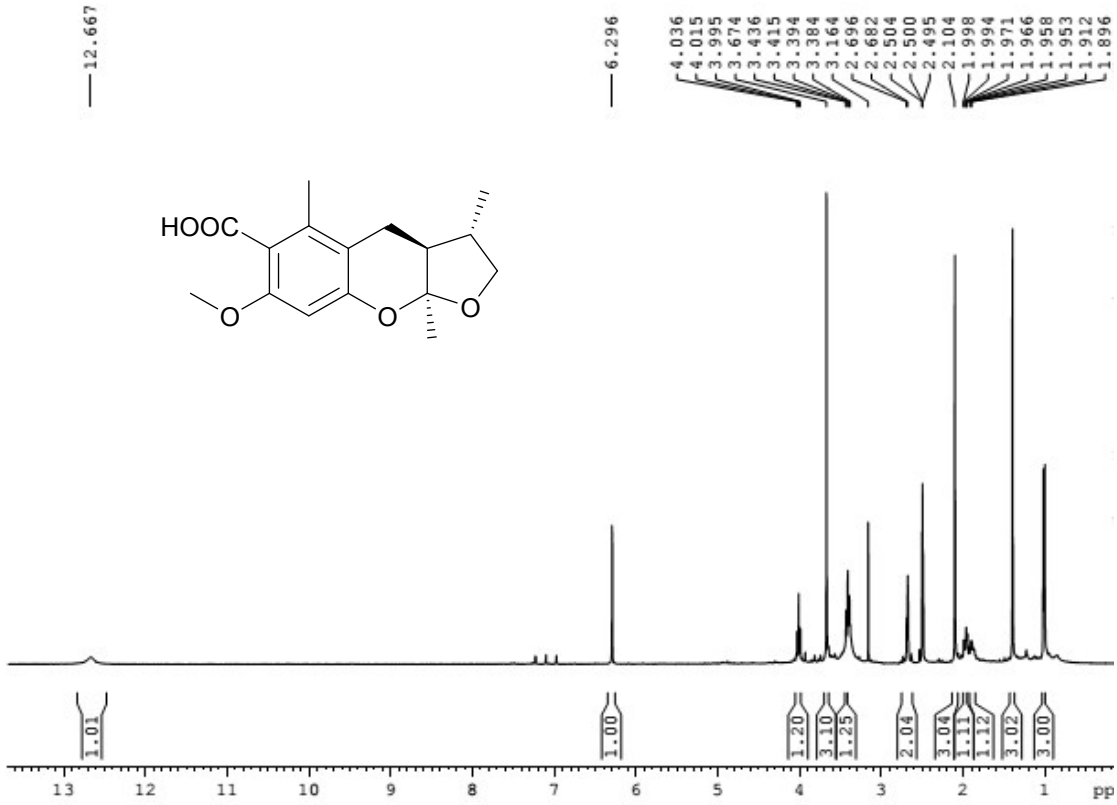

Figure S5. The ^{13}C-NMR spectrum of compound **1**

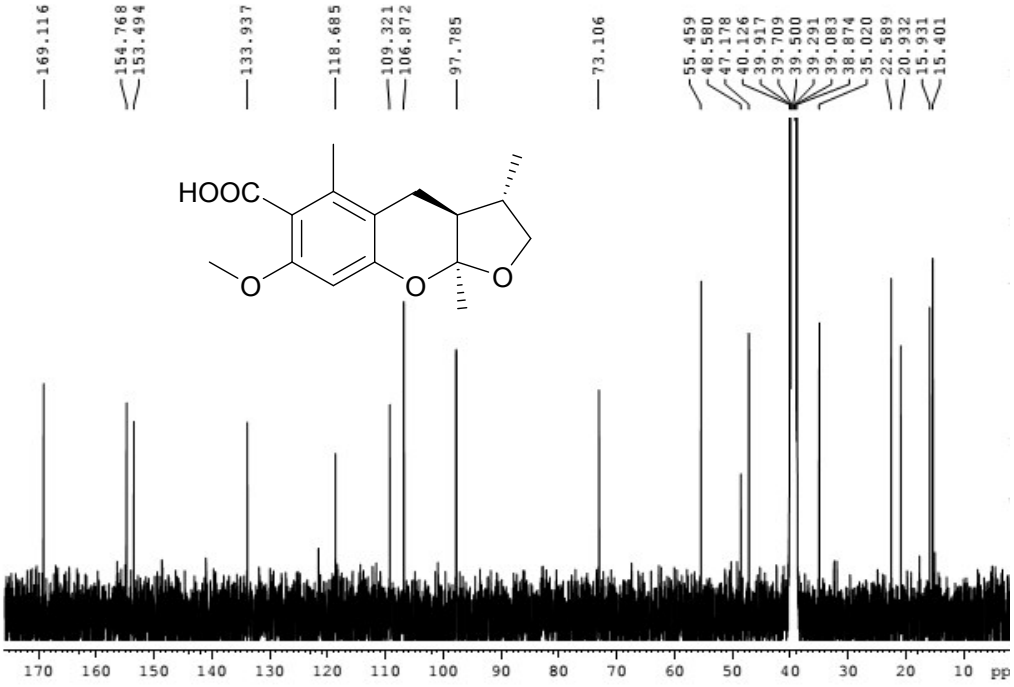

Figure S6. The HSQC spectrum of compound **1**

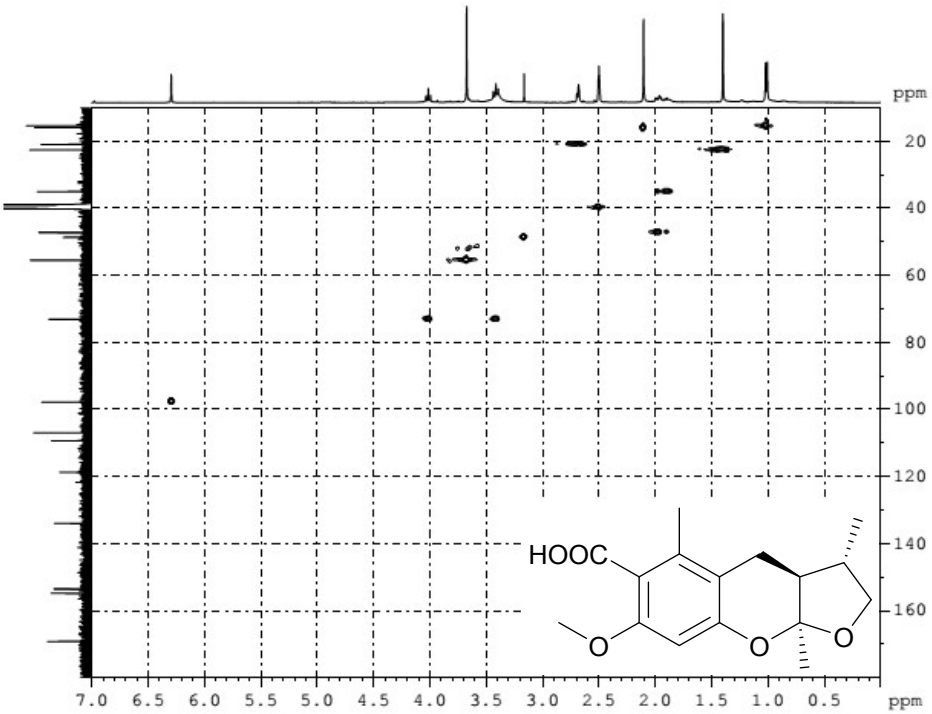

Figure S7. The HMBC spectrum of compound **1**

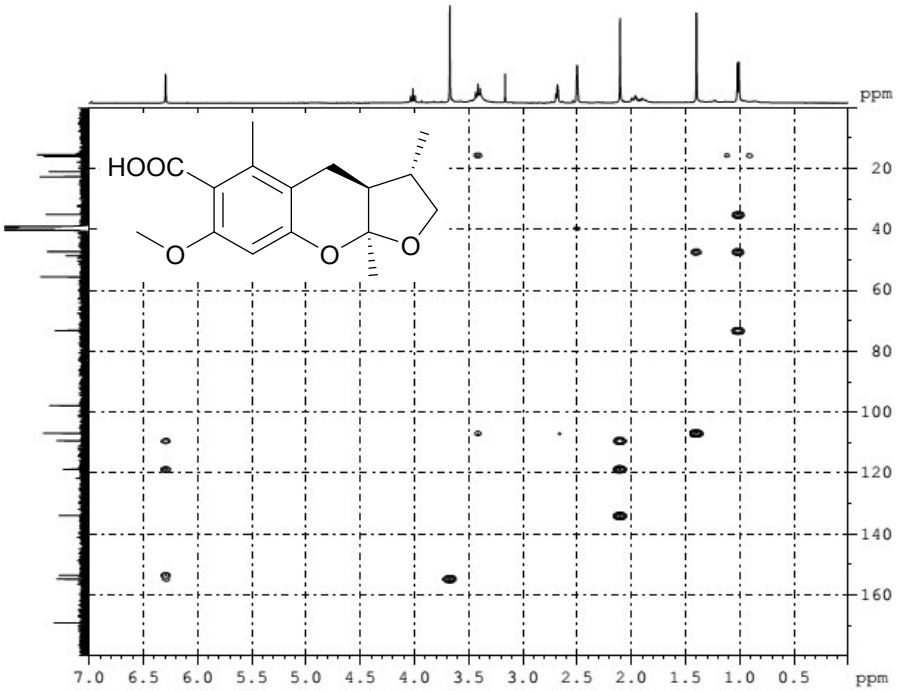

Figure S8. The NOESY spectrum of compound **1**

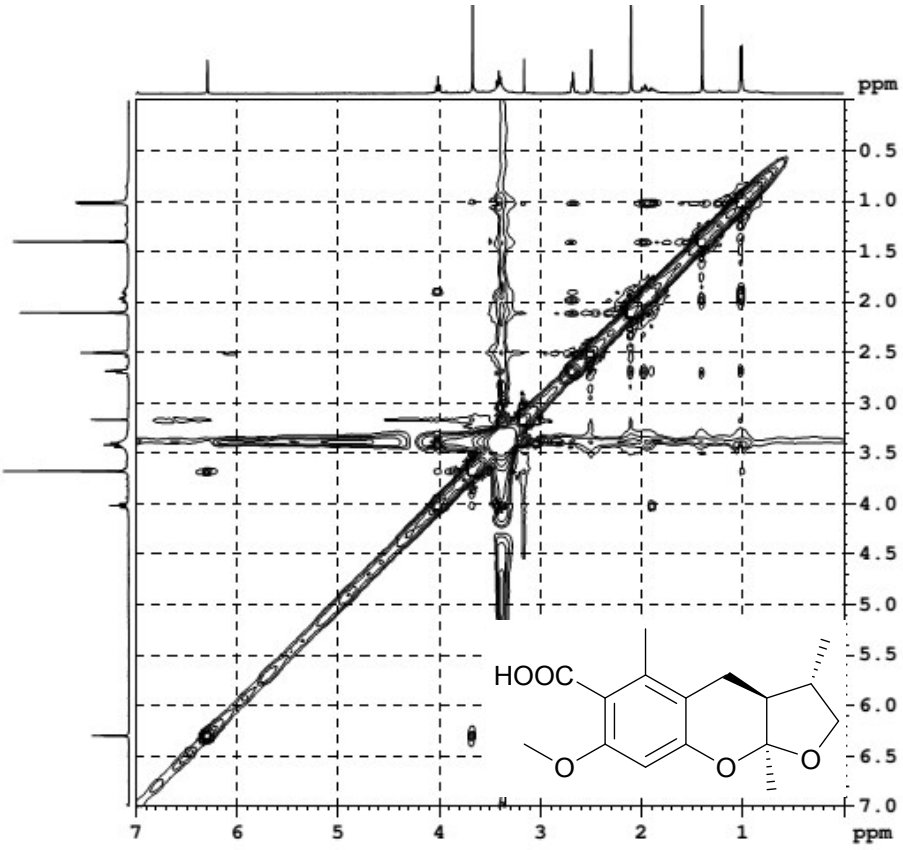

Computational details for ECD of compound **1**

Computational method

The Spartan 14.0 (Wavefunction Inc., Irvine, CA, USA) searches using molecular mechanics MMFF were performed for **1a**, which gave 6 conformers. The only low-energy conformer of **1a** accounting for more than 30% Boltzmann distribution was further optimized and analysed frequency in Gaussian 09 program package,[1] using the density functional theory (DFT) at the B3LYP/6-31G (d, p) level and the same way in the methanol, resulted in no imaginary frequencies. Solvent effects were taken into consideration by using the conductor polarizable continuum model (CPCM). The conformer of **1a** was calculated electronic circular dichroism (ECD) by the time-dependent density functional theory (TD-DFT) method at the B3LYP/6-31G (d, p) level with the CPCM model in methanol solution. The calculated ECD curve of the **1a** was generated using SpecDis 1.51 [2-3] with $\sigma = 0.27$ eV at 21 nm shift.

References

[1] Frisch, M. J.; Trucks, G. W.; Schlegel, H. B.; Scuseria, G. E.; Robb, M. A.; Cheeseman, J. R.; Scalmani, G.; Barone, V.; Mennucci, B.; Petersson, G. A.; Nakatsuji, H.; Caricato, M.; Li, X.; Hratchian, H. P.; Izmaylov, A. F.; Bloino, J.; Zheng, G.; Sonnenberg, J. L.; Hada, M.; Ehara, M.; Toyota, K.; Fukuda, R.; Hasegawa, J.; Ishida, M.; Nakajima, T.; Honda, Y.; Kitao, O.; Nakai, H.; Vreven, T.; Montgomery, J. A., Jr.; Peralta, J. E.; Ogliaro, F.; Bearpark, M.; Heyd, J. J.; Brothers, E.; Kudin, K. N.; Staroverov, V. N.; Kobayashi, R.; Normand, J.; Raghavachari, K.; Rendell, A.; Burant, J. C.; Iyengar, S. S.; Tomasi, J.; Cossi, M.; Rega, N.; Millam, J. M.; Klene, M.; Knox, J. E.; Cross, J. B.; Bakken, V.; Adamo, C.; Jaramillo, J.; Gomperts, R.; Stratmann, R. E.; Yazyev, O.; Austin, A. J.; Cammi, R.; Pomelli, C.; Ochterski, J. W.; Martin, R. L.; Mo ro ku ma , K . ; Z a kr ze w sk i, V. G .; Vo th, G. A.; Sa lv a d or , P .; Dannenberg,J.J.; Dapprich,S.; Daniels,A.D.;Farkas,O; Foresman, J. B.; Ortiz, J. V.; Cioslowski, J.; Fox, D. J. Gaussian 09, Revision C1; Gaussian, Inc.: Wallingford, CT, 2010.

[2]. Bruhn, T.; Hemberger, Y.; Schaumlöffel, A.; Bringmann, G. *Spec Dis*, version 1.51, University of Würzburg, Germany, 2010.

[3] Bruhn, T.; Schaumlöffel, A.; Hemberger, Y.; Bringmann, G. Quantifying the Comparison of Calculated and Experimental Electronic Circular Dichroism Spectra, Chirality 2013, 25, 243–249.

Table S1 Energy analysis of **1a**

Label	MMFF	
	rel. E(Kal/mol)	Boltzmann Dist.
1a	0.00	0.427

Table S2 Computational methods for ECD of **1a**

Standard orientation:

Center Number	Atomic Number	Atomic Type	Coordinates (Angstroms) X	Y	Z
1	6	0	2.294137	-0.406386	0.062038
2	6	0	2.126481	0.982748	-0.158015
3	6	0	0.861601	1.554620	-0.094348
4	6	0	-0.248220	0.744174	0.179380
5	6	0	-0.117418	-0.633984	0.391622
6	6	0	1.174082	-1.206569	0.351978
7	8	0	-1.446254	1.400083	0.197842
8	6	0	-2.636787	0.749775	0.740159
9	6	0	-2.649261	-0.731742	0.348084
10	6	0	-1.347691	-1.467210	0.678526
11	8	0	-3.721036	1.316058	0.062951
12	6	0	-3.948854	0.599629	-1.171985
13	6	0	-3.040237	-0.649867	-1.145088
14	8	0	3.263496	1.701427	-0.373652
15	1	0	0.694824	2.614734	-0.231516
16	1	0	0.768737	-3.259890	-0.186958
17	6	0	3.160123	3.104572	-0.583513
18	1	0	4.180854	3.453195	-0.744171
19	6	0	1.304545	-2.696289	0.586816
20	1	0	2.553019	3.331635	-1.468205
21	6	0	3.666617	-0.992807	0.012435
22	1	0	2.735254	3.609122	0.292990
23	6	0	-2.734798	1.082224	2.218209
24	6	0	-3.707906	-1.909243	-1.700624
25	8	0	4.194676	-1.633874	0.902924
26	8	0	4.295172	-0.772953	-1.168893
27	1	0	-3.476358	-1.200716	0.896873
28	1	0	-1.358853	-1.764860	1.737313

29	1	0	-1.317234	-2.406920	0.114382
30	1	0	-3.730940	1.261661	-2.016591
31	1	0	-5.012181	0.333959	-1.199067
32	1	0	-2.134487	-0.445051	-1.728972
33	1	0	2.341045	-3.026416	0.598093
34	1	0	0.862670	-2.977064	1.549638
35	1	0	-1.855647	0.712459	2.753897
36	1	0	-2.789422	2.166542	2.342325
37	1	0	-3.632682	0.629657	2.648337
38	1	0	-3.035657	-2.772837	-1.648718
39	1	0	-3.988131	-1.778607	-2.751838
40	1	0	-4.617527	-2.154360	-1.138953
41	1	0	5.185799	-1.154034	-1.082279

Table S3 2D Structures of **1a** and **1b**

label	structure
1a	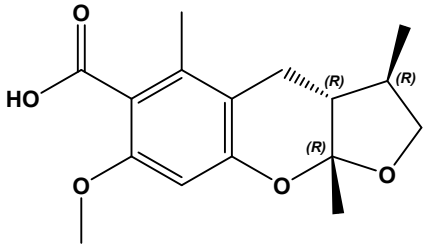
1b	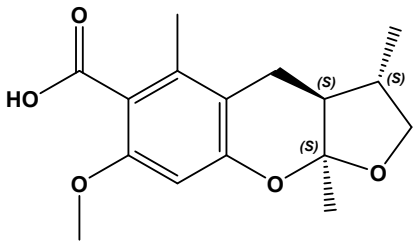

Figure S9. B3LYP/6-31 G* optimized lowest energy 3D conformer of **1**

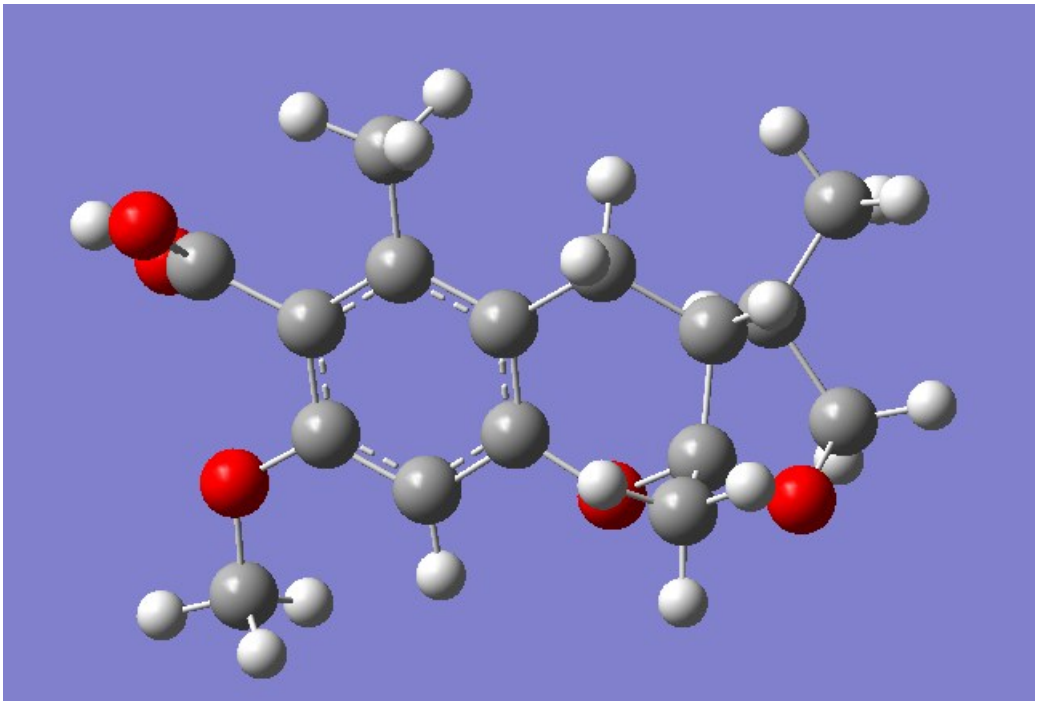

Figure S10. Experimental and suitable calculated ECD spectra of **1**

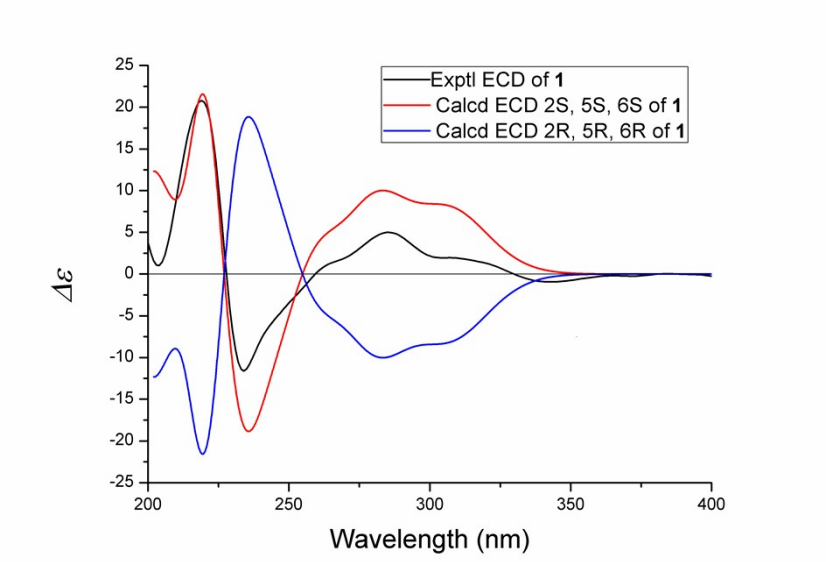

6. The spectra of Phomeketale B (2)

Figure S11. The UV spectrum of compound **2**

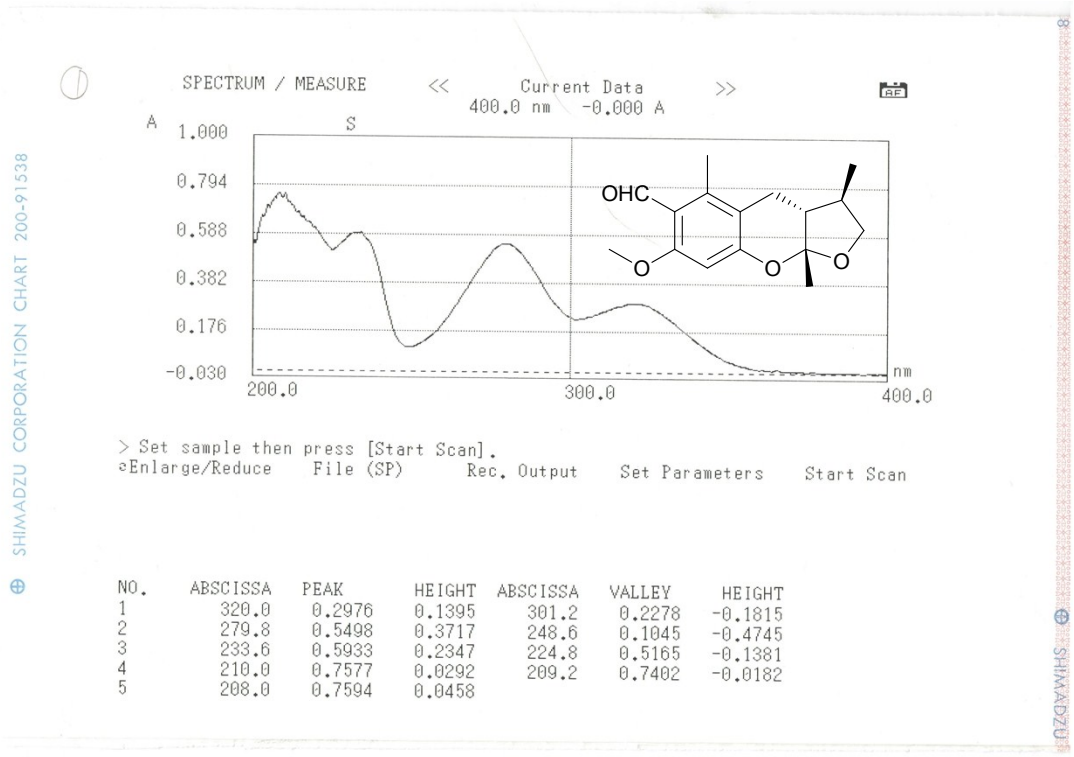

Figure S12. The IR spectrum of compound **2**

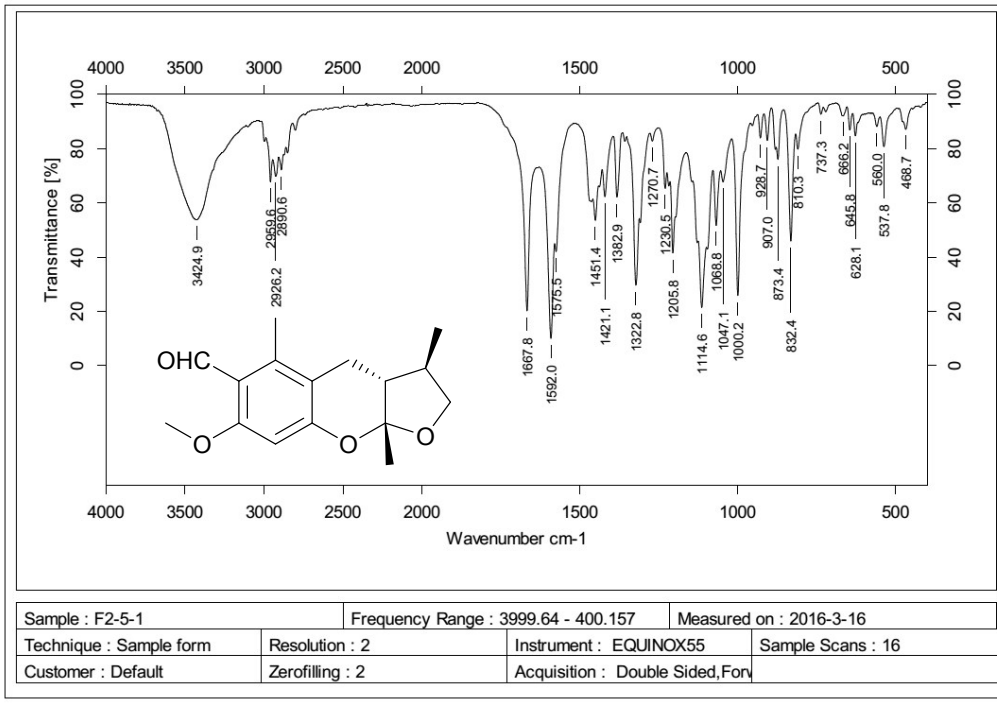

Figure S13. The HR-ESI-MS spectrum of compound **2**

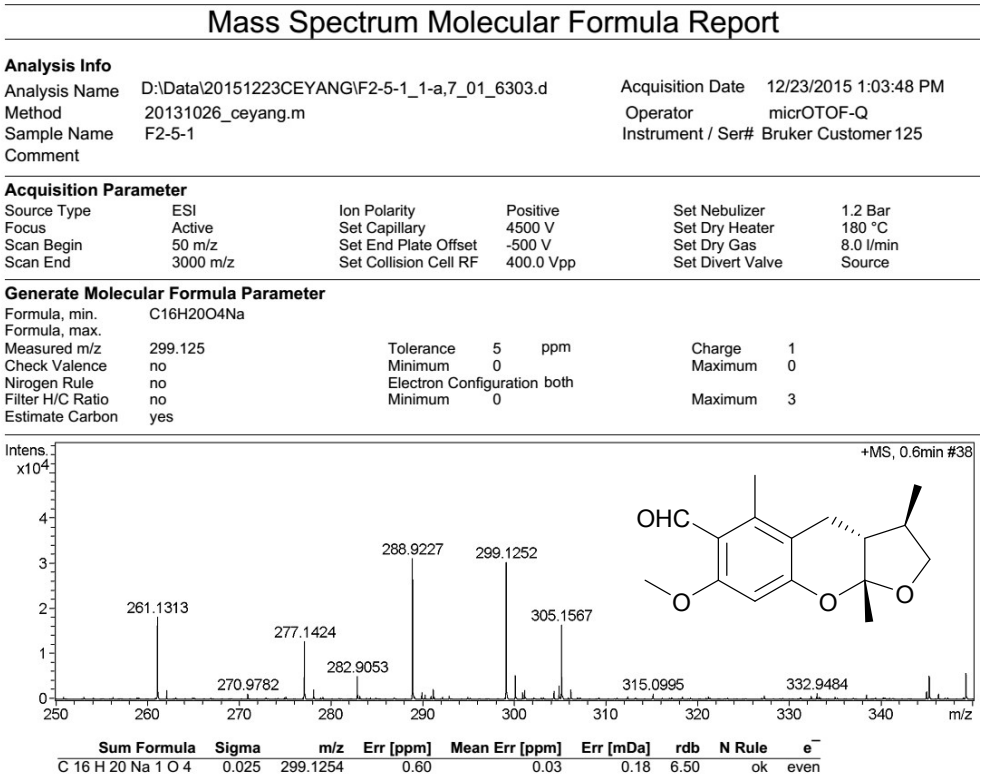

Mass Spectrum Molecular Formula Report

Analysis Info

Analysis Name	D:\Data\20151223CEYANG\F2-5-1_1-a,7_01_6303.d	Acquisition Date	12/23/2015 1:03:48 PM
Method	20131026_ceyang.m	Operator	micrOTOF-Q
Sample Name	F2-5-1	Instrument / Ser#	Bruker Customer 125
Comment			

Acquisition Parameter

Source Type	ESI	Ion Polarity	Positive	Set Nebulizer	1.2 Bar
Focus	Active	Set Capillary	4500 V	Set Dry Heater	180 °C
Scan Begin	50 m/z	Set End Plate Offset	-500 V	Set Dry Gas	8.0 l/min
Scan End	3000 m/z	Set Collision Cell RF	400.0 Vpp	Set Divert Valve	Source

Generate Molecular Formula Parameter

Formula, min.	C16H20O4Na						
Formula, max.							
Measured m/z	299.125	Tolerance	5	ppm	Charge	1	
Check Valence	no	Minimum	0		Maximum	0	
Nirogen Rule	no	Electron Configuration	both				
Filter H/C Ratio	no	Minimum	0		Maximum	3	
Estimate Carbon	yes						

Sum Formula	Sigma	m/z	Err [ppm]	Mean Err [ppm]	Err [mDa]	rdb	N Rule	e⁻
C 16 H 20 Na 1 O 4	0.025	299.1254	0.60	0.03	0.18	6.50	ok	even

Figure S14. The ^{1}H-NMR spectrum of compound **2**

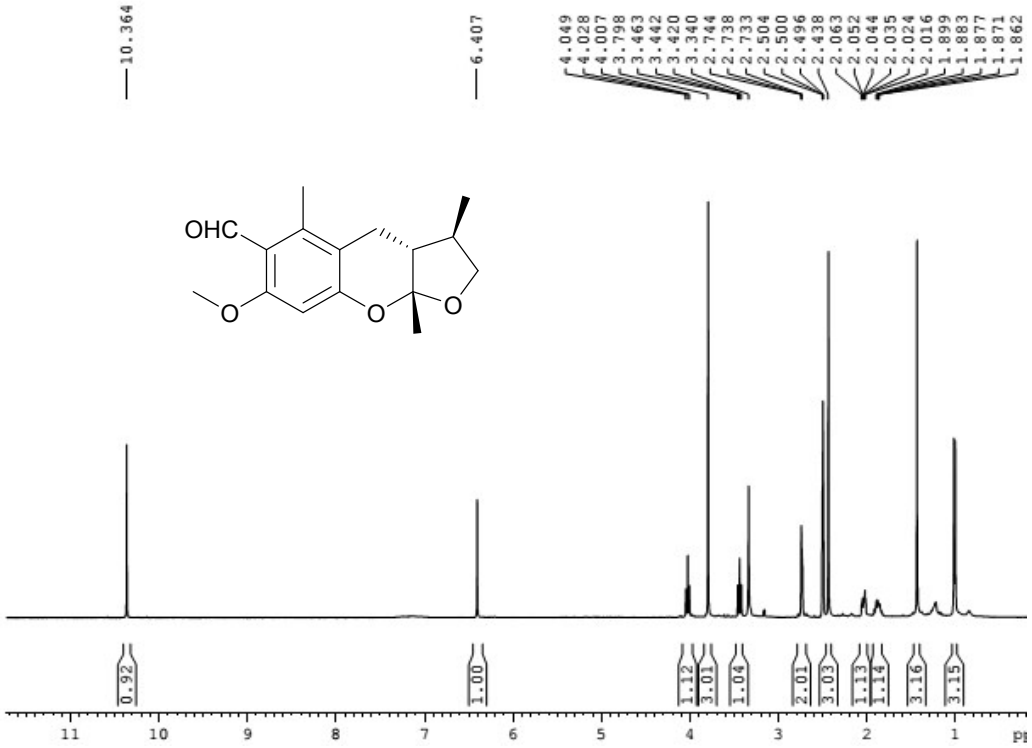

Figure S15. The ^{13}C-NMR spectrum of compound **2**

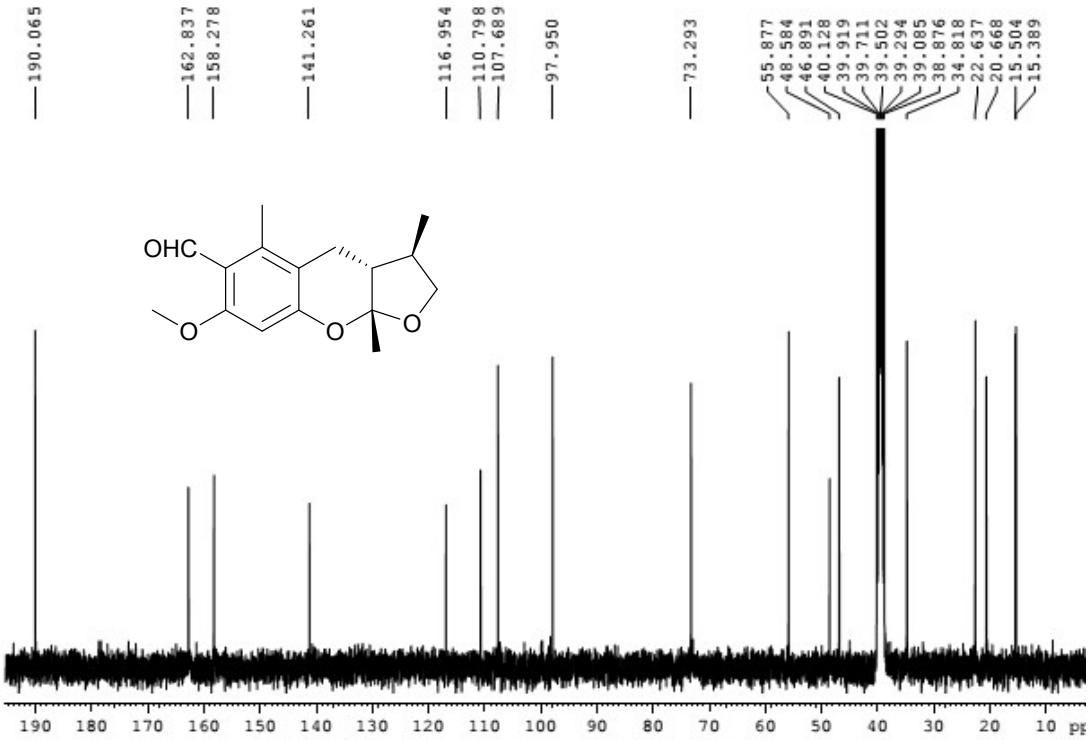

Figure S16. The HSQC spectrum of compound **2**

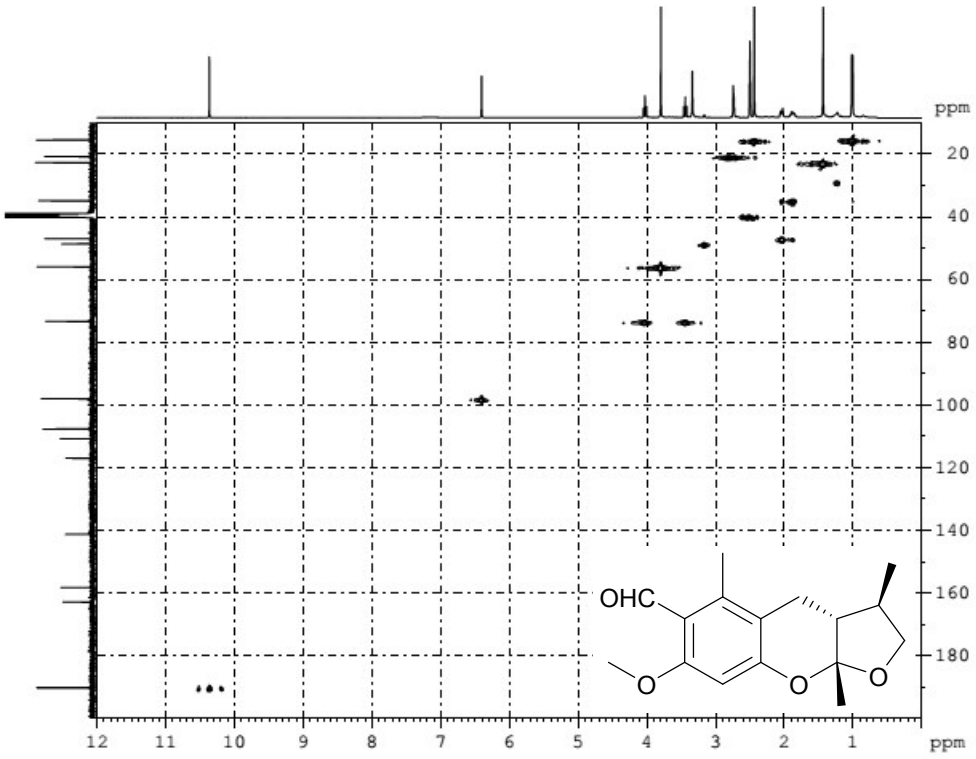

Figure S17. The HMBC spectrum of compound **2**

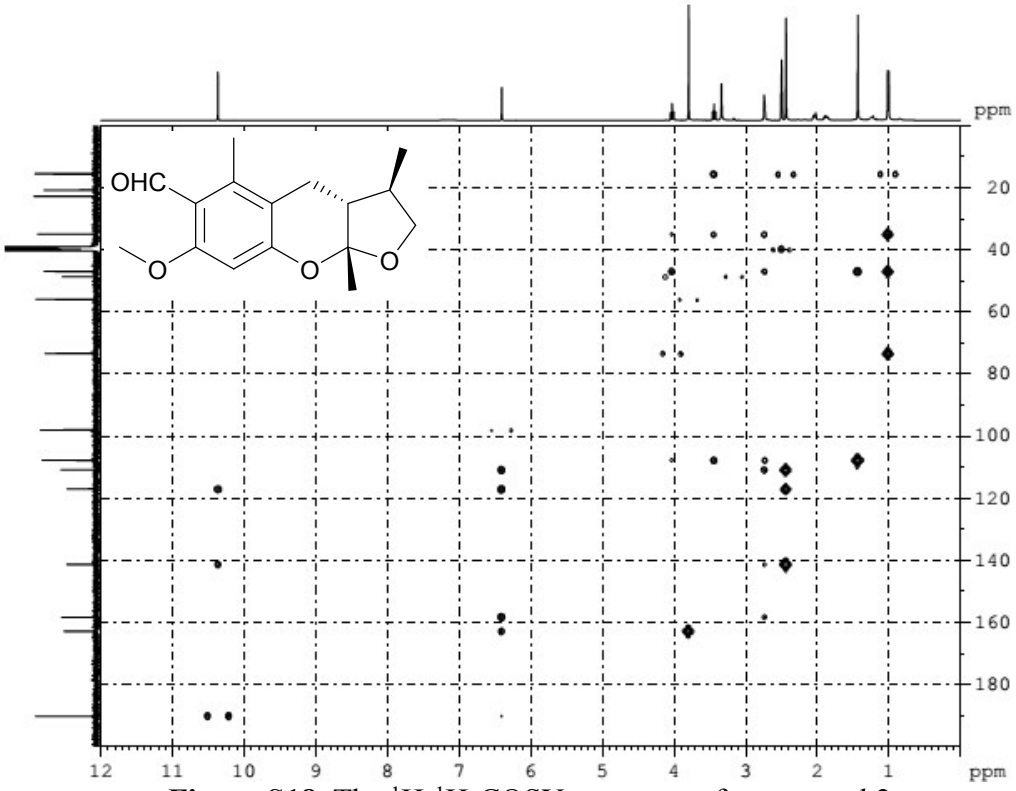

Figure S18. The ^{1}H-^{1}H-COSY spectrum of compound **2**

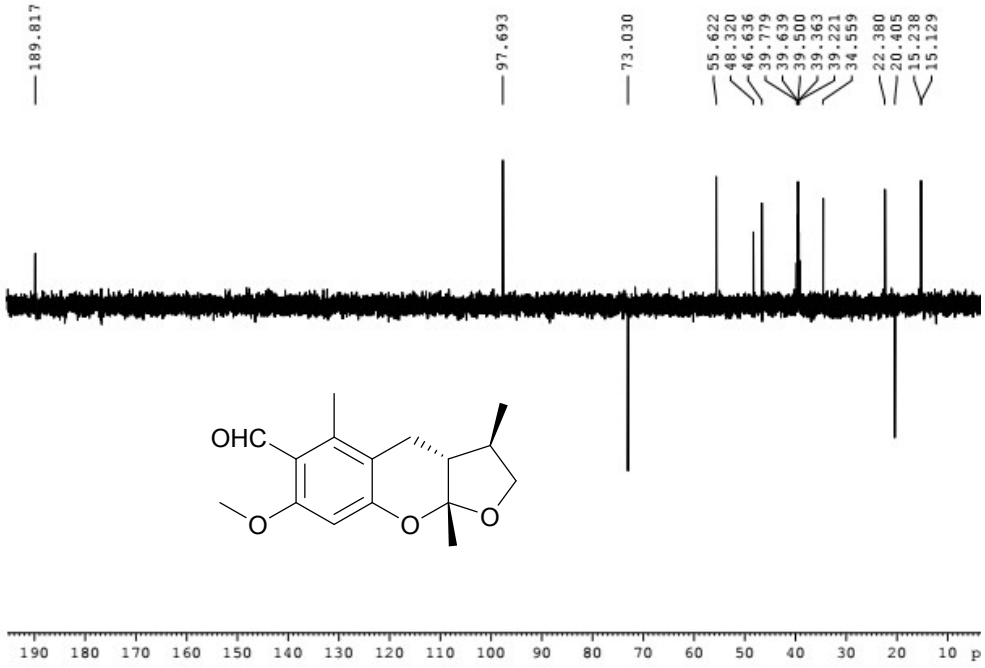

Figure S19. The DEPT-135 spectrum of compound **2**

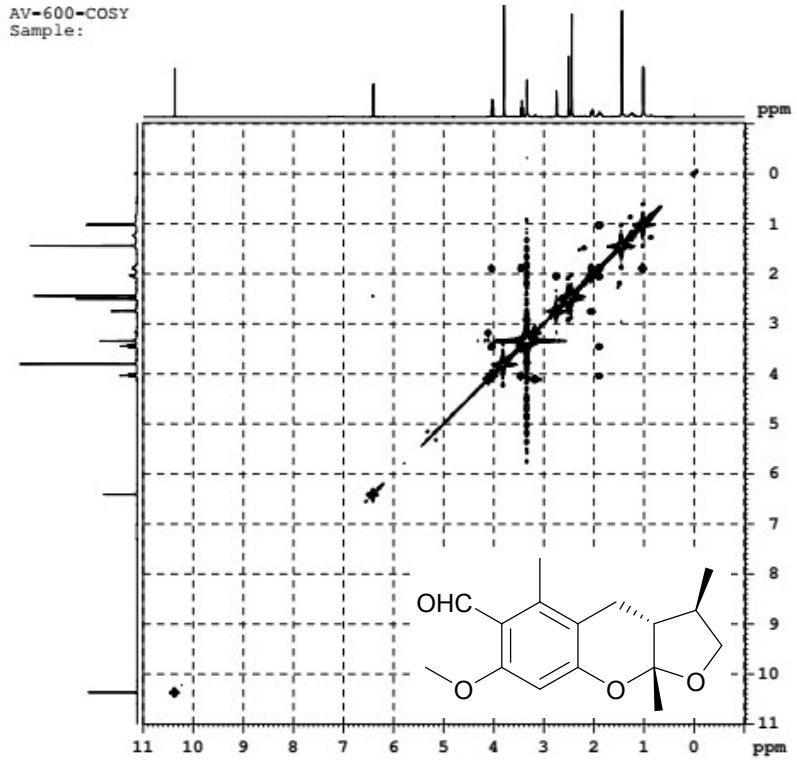

Figure S20. The NOESY spectrum of compound **2**

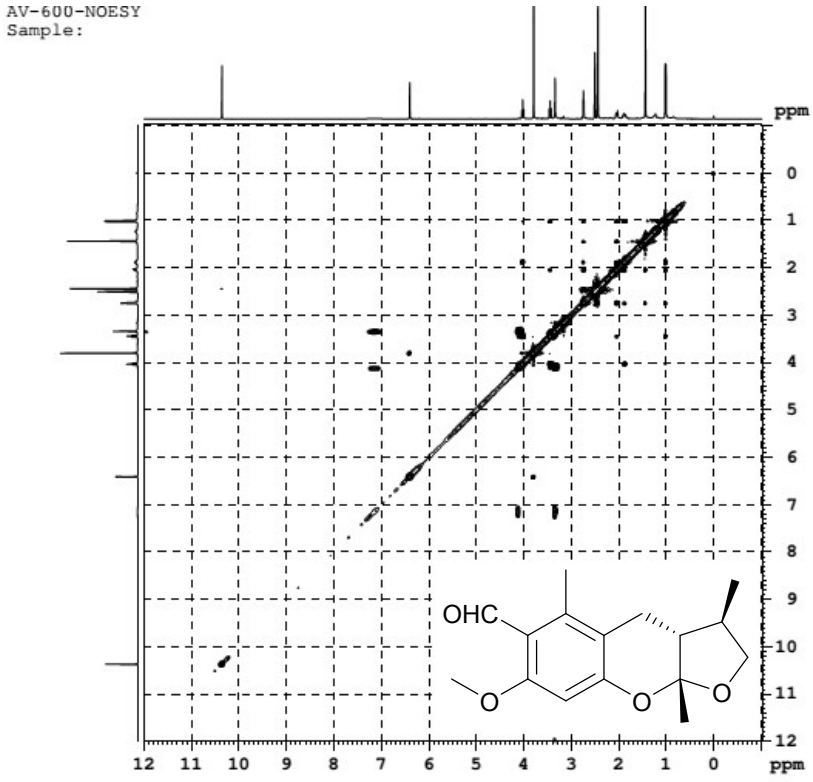

Computational details for ECD of compound **2**

Computational methods

The Spartan 14.0 (Wavefunction Inc., Irvine, CA, USA) searches using molecular mechanics MMFF were performed for **2a**, which gave 6 conformers. The only low-energy conformer of **2a** accounting for more than 5% Boltzmann distribution was further optimized and analysed frequency in Gaussian 09 program package, using the density functional theory (DFT) at the B3LYP/6-31G (d, p) level and the same way in the methanol, resulted in no imaginary frequencies. Solvent effects were taken into consideration by using the conductor polarizable continuum model (CPCM). The conformer of **2a** was calculated electronic circular dichroism (ECD) by the time-dependent density functional theory (TD-DFT) method at the B3LYP/6-31G (d, p) level with the CPCM model in methanol solution. The calculated ECD curve of the **2a** was generated using SpecDis 1.51 with $\sigma = 0.16$ eV at 0 nm shift.

Table S4 Energy analysis of **2a**

Label	MMFF	
	rel. E(Kal/mol)	Boltzmann Dist.
2a	0.00	1.000

Table S5 Computational methods for ECD of **2a**

Standard orientation:

Center Number	Atomic Number	Atomic Type	Coordinates (Angstroms) X	Y	Z
1	6	0	-2.616884	0.648157	0.016788
2	6	0	-2.601476	-0.773404	-0.116870
3	6	0	-1.400491	-1.457594	-0.293236
4	6	0	-0.220699	-0.720216	-0.350359
5	6	0	-0.183428	0.683250	-0.259158
6	6	0	-1.388807	1.376511	-0.064693
7	8	0	0.943667	-1.412180	-0.551714
8	6	0	2.069731	-1.005640	0.274168
9	6	0	2.308533	0.530849	0.234316

10	6	0	1.183514	1.287800	-0.502211
11	8	0	3.186902	-1.616483	-0.344676
12	6	0	4.302353	-0.711473	-0.261720
13	6	0	3.701176	0.686420	-0.430596
14	8	0	-3.799370	-1.412141	-0.046110
15	1	0	-1.348971	-2.535839	-0.371987
16	1	0	-1.840293	3.213163	0.980678
17	1	0	-4.770732	0.576930	0.236021
18	6	0	-3.844978	-2.836450	-0.189108
19	1	0	-3.454713	-3.144593	-1.165132
20	6	0	-1.402437	2.885380	0.032944
21	1	0	-3.284276	-3.329237	0.612579
22	6	0	-3.923541	1.280186	0.217097
23	1	0	-4.900269	-3.100158	-0.114806
24	6	0	1.862370	-1.577172	1.674739
25	6	0	4.564572	1.813663	0.139155
26	8	0	-4.152374	2.484565	0.362021
27	1	0	2.353820	0.891110	1.268905
28	1	0	1.229501	2.342366	-0.228462
29	1	0	1.384187	1.239760	-1.582831
30	1	0	5.007303	-0.992517	-1.047904
31	1	0	4.798772	-0.821285	0.714289
32	1	0	3.552109	0.860077	-1.504567
33	1	0	-0.400961	3.307105	-0.047982
34	1	0	-2.023341	3.325186	-0.754482
35	1	0	0.982610	-1.135157	2.154761
36	1	0	1.730728	-2.662157	1.615079
37	1	0	2.735393	-1.359605	2.299393
38	1	0	4.082420	2.788105	-0.000728
39	1	0	5.540505	1.851861	-0.359927
40	1	0	4.738568	1.673192	1.213389

Table S6 2D Structures of **2a**

label	structure
2a	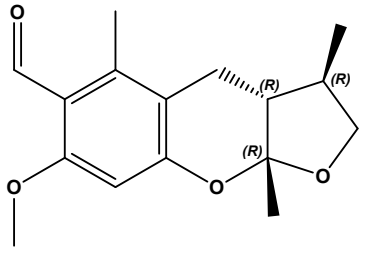

2b

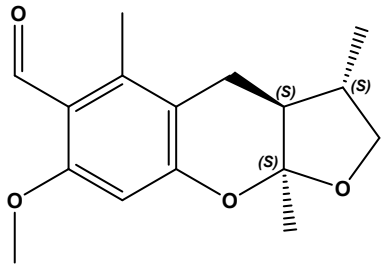

Figure S21. B3LYP/6-31 G* optimized lowest energy 3D conformer of **2**

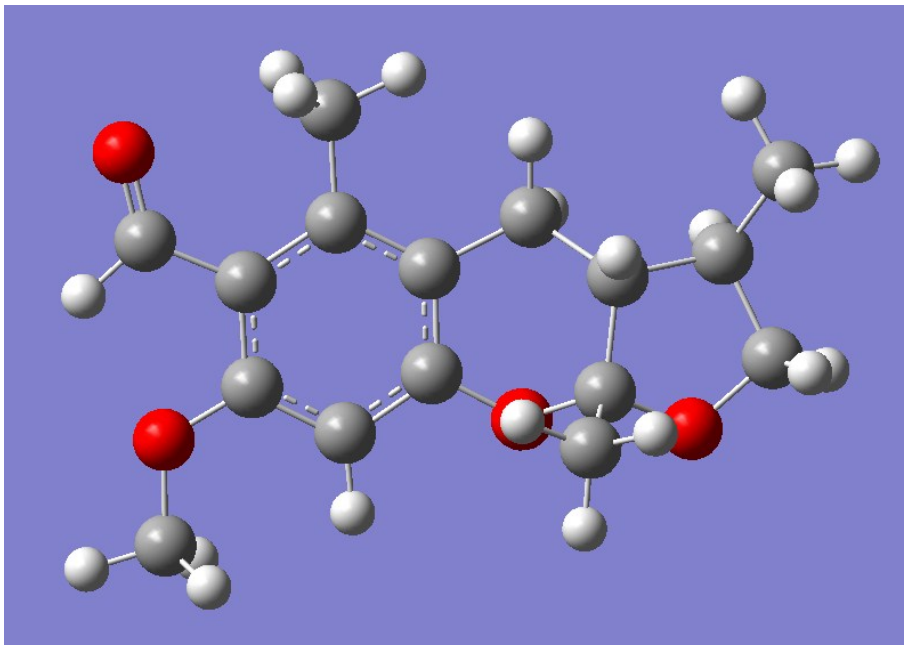

Figure S22. Experimental and suitable calculated ECD spectra of **2**

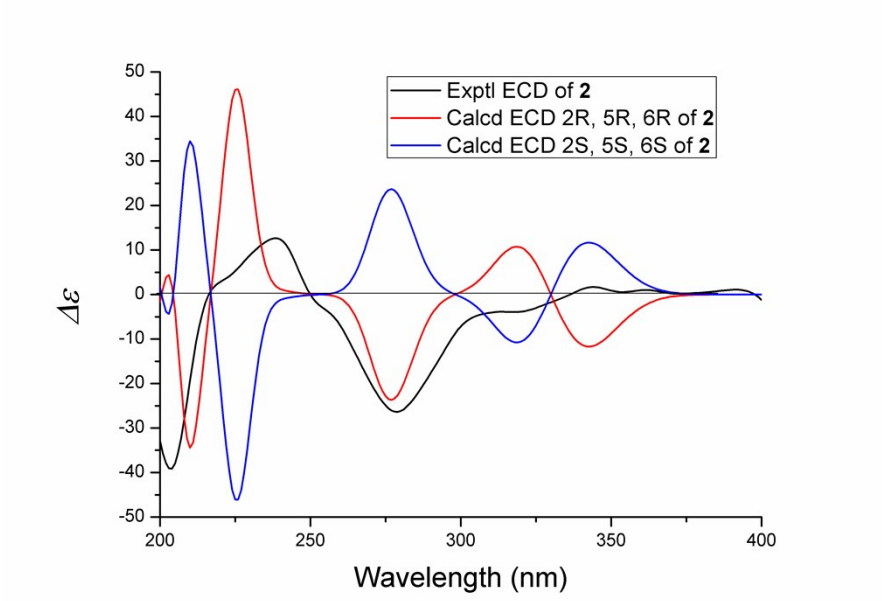

7. The spectra of Phomeketale C (3)

Figure S23. The UV spectrum of compound **3**

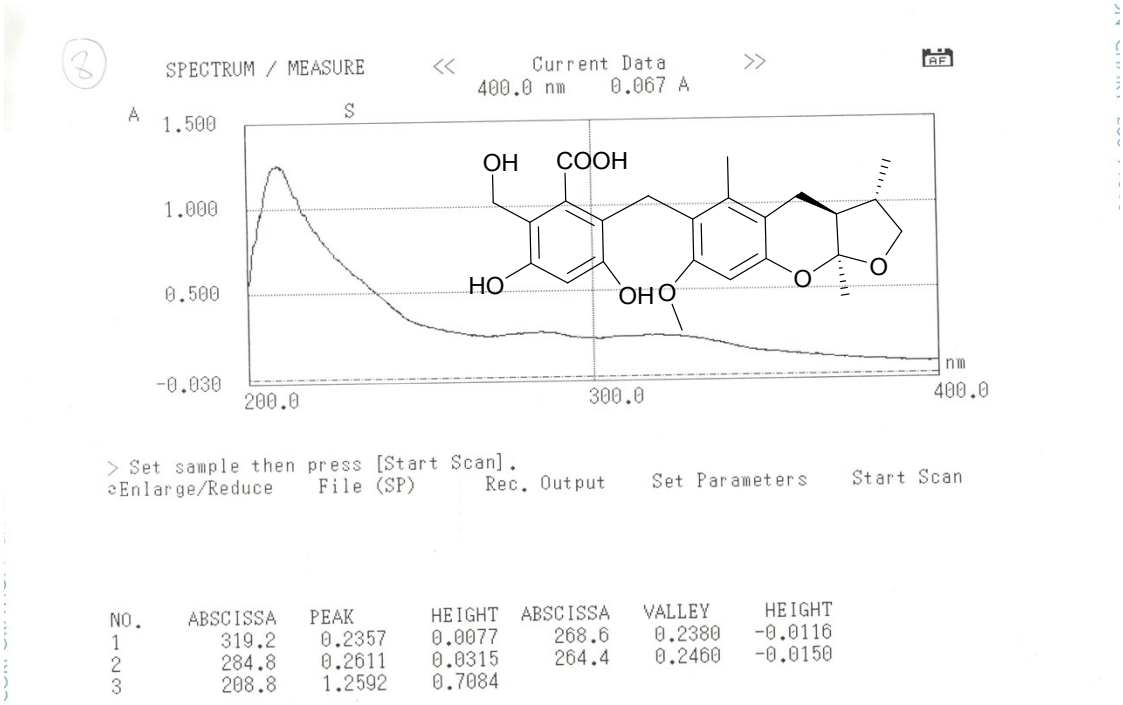

Figure S24. The IR spectrum of compound **3**

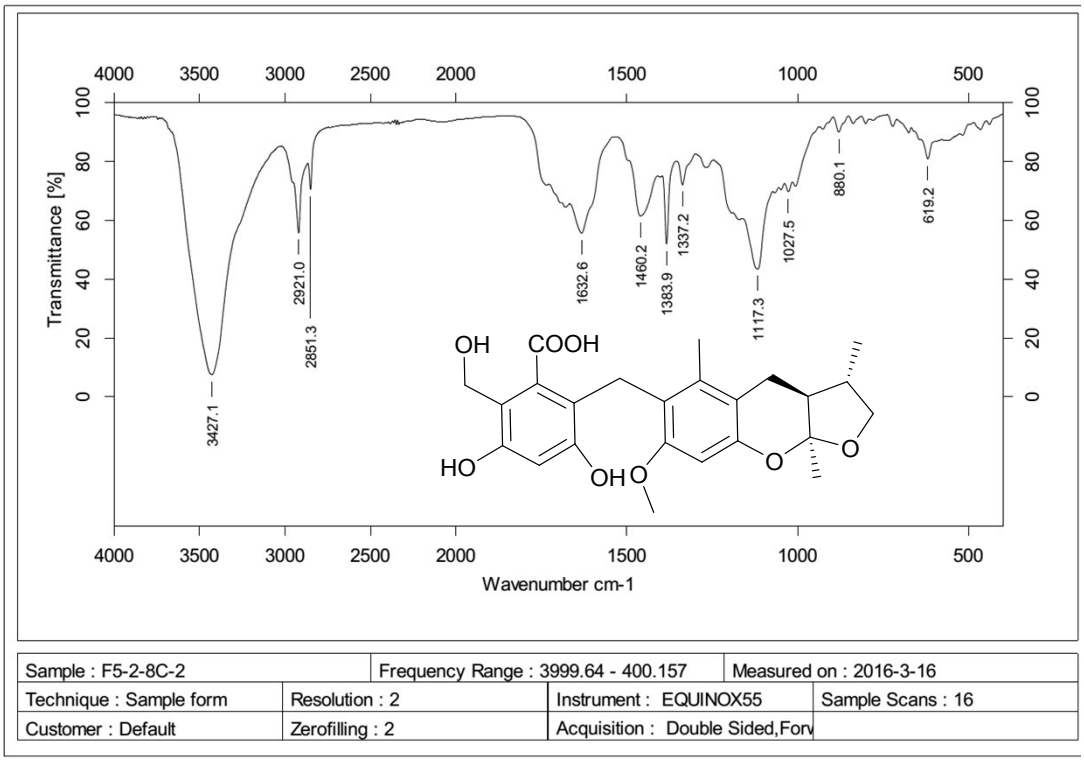

Figure S25. The HR-ESI-MS spectrum of compound **3**

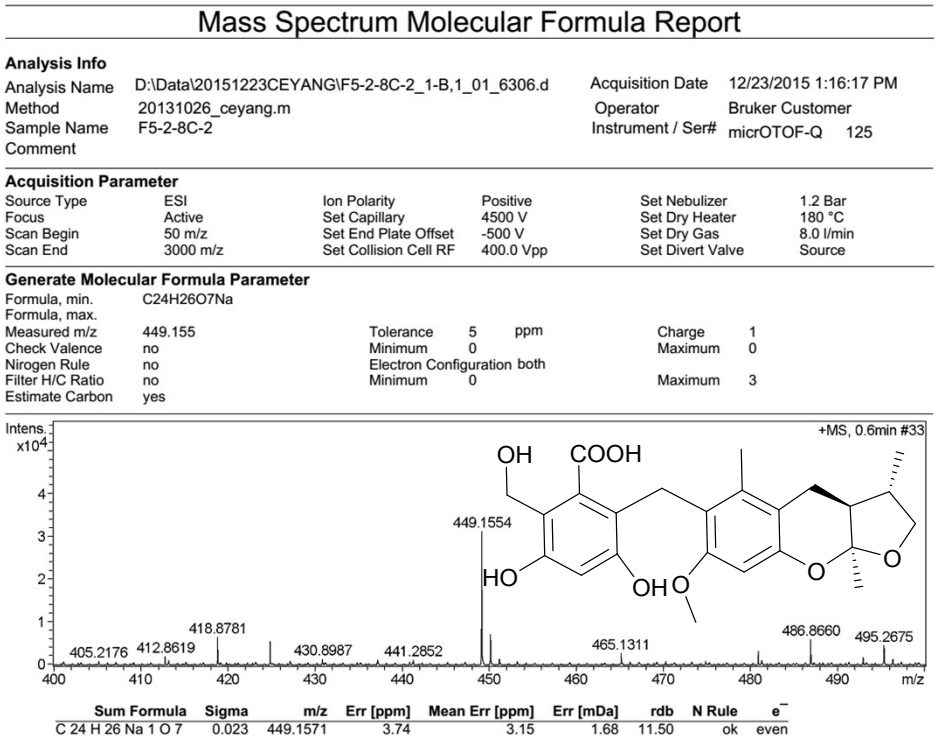

Mass Spectrum Molecular Formula Report

Analysis Info

Analysis Name	D:\Data\20151223CEYANG\F5-2-8C-2_1-B,1_01_6306.d	Acquisition Date	12/23/2015 1:16:17 PM
Method	20131026_ceyang.m	Operator	Bruker Customer
Sample Name	F5-2-8C-2	Instrument / Ser#	micrOTOF-Q 125
Comment			

Acquisition Parameter

Source Type	ESI	Ion Polarity	Positive	Set Nebulizer	1.2 Bar
Focus	Active	Set Capillary	4500 V	Set Dry Heater	180 °C
Scan Begin	50 m/z	Set End Plate Offset	-500 V	Set Dry Gas	8.0 l/min
Scan End	3000 m/z	Set Collision Cell RF	400.0 Vpp	Set Divert Valve	Source

Generate Molecular Formula Parameter

Formula, min.	C24H26O7Na				
Formula, max.					
Measured m/z	449.155	Tolerance	5 ppm	Charge	1
Check Valence	no	Minimum	0	Maximum	0
Nirogen Rule	no	Electron Configuration	both		
Filter H/C Ratio	no	Minimum	0	Maximum	3
Estimate Carbon	yes				

Sum Formula	Sigma	m/z	Err [ppm]	Mean Err [ppm]	Err [mDa]	rdb	N Rule	e⁻
C 24 H 26 Na 1 O 7	0.023	449.1571	3.74	3.15	1.68	11.50	ok	even

Figure S26. The ^{1}H-NMR spectrum of compound **3**

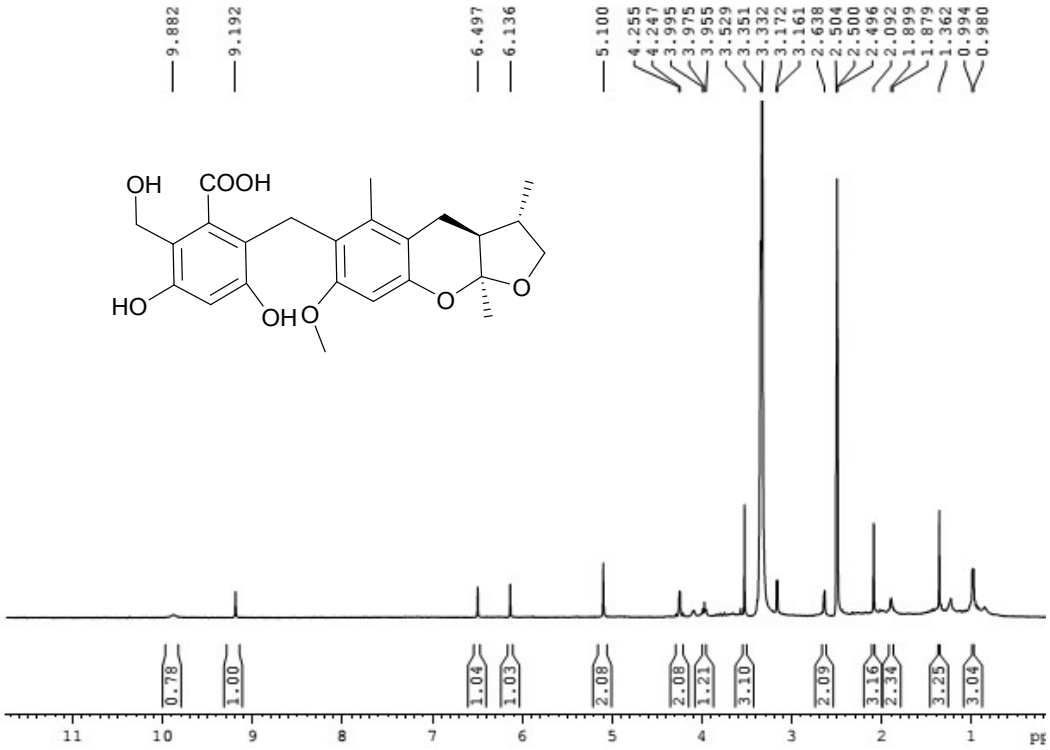

Figure S27. The ^{13}C-NMR spectrum of compound **3**

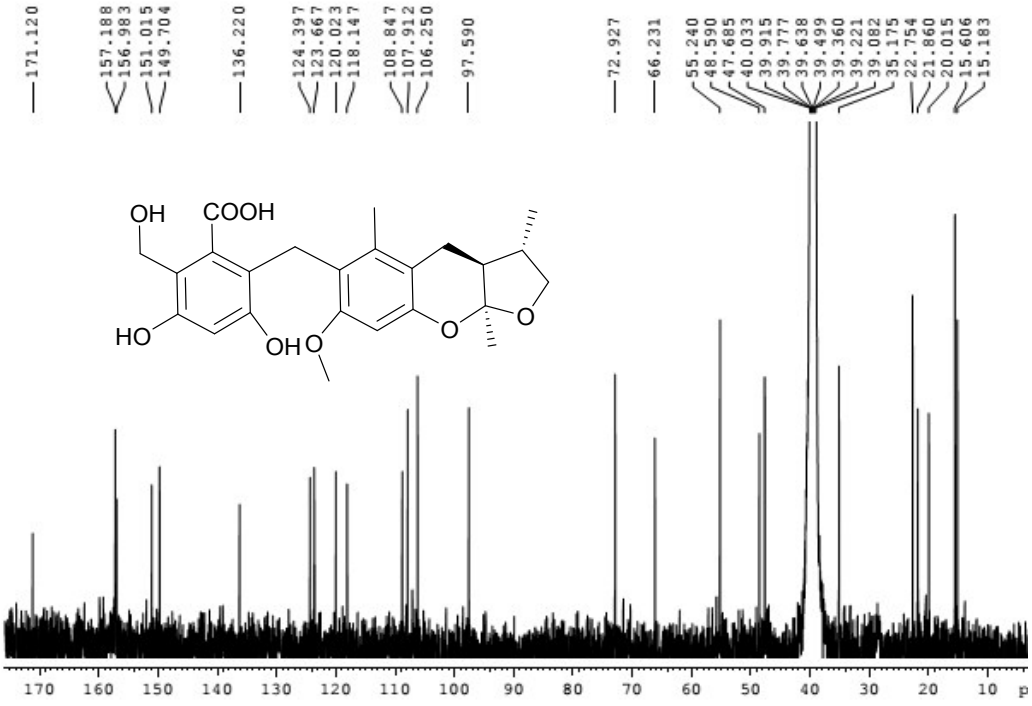

Figure S28. The HMQC spectrum of compound **3**

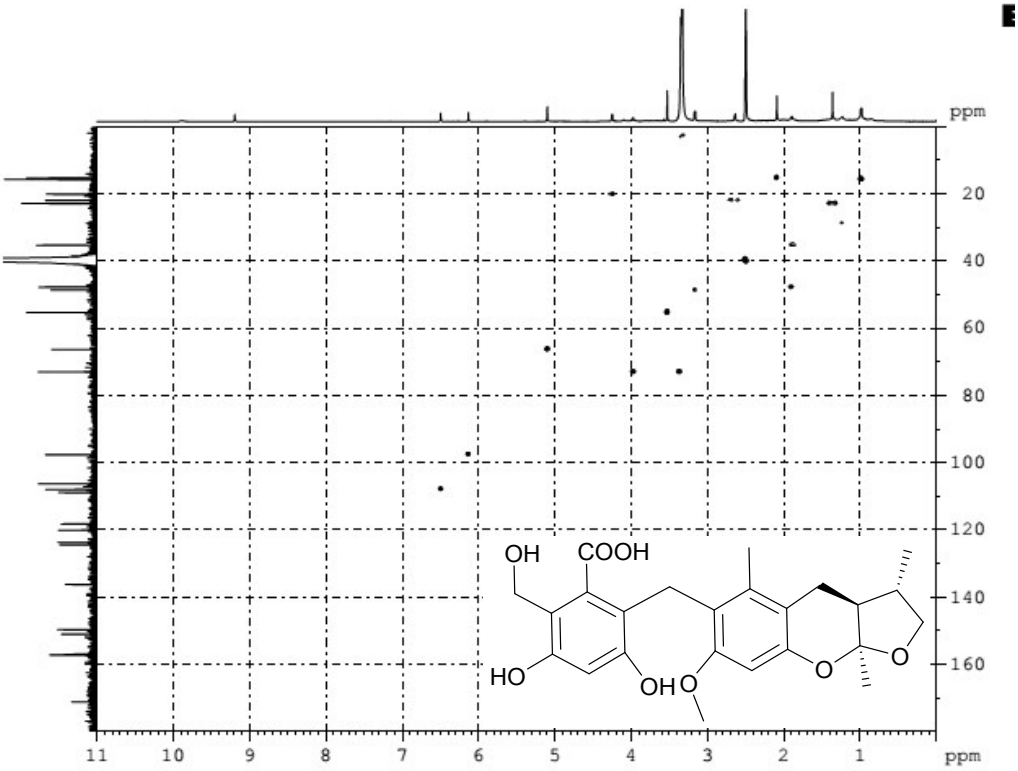

Figure S29. The HMBC spectrum of compound **3**

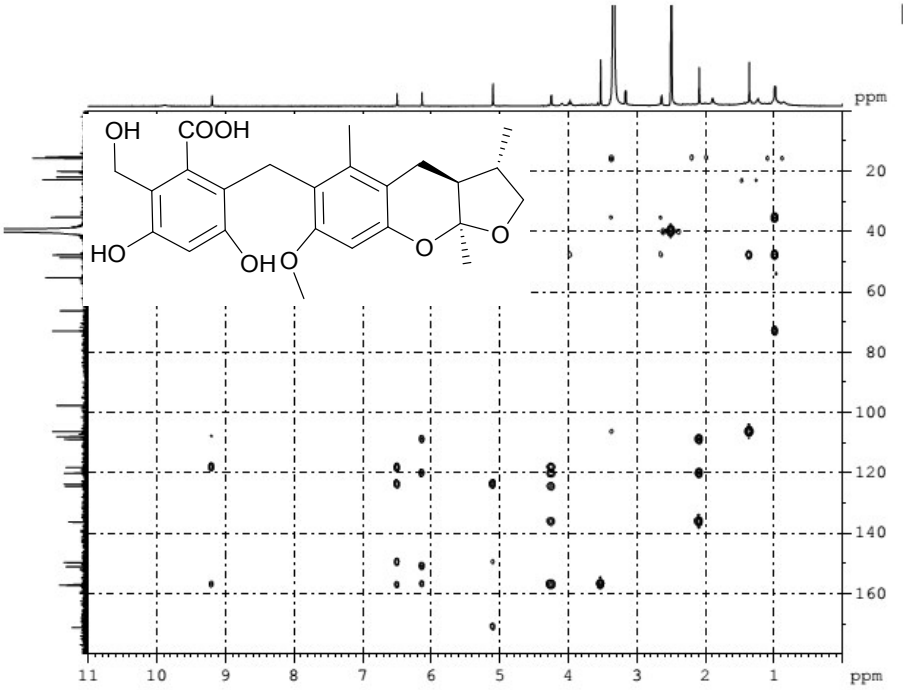

Figure S30. The NOESY spectrum of compound **3**

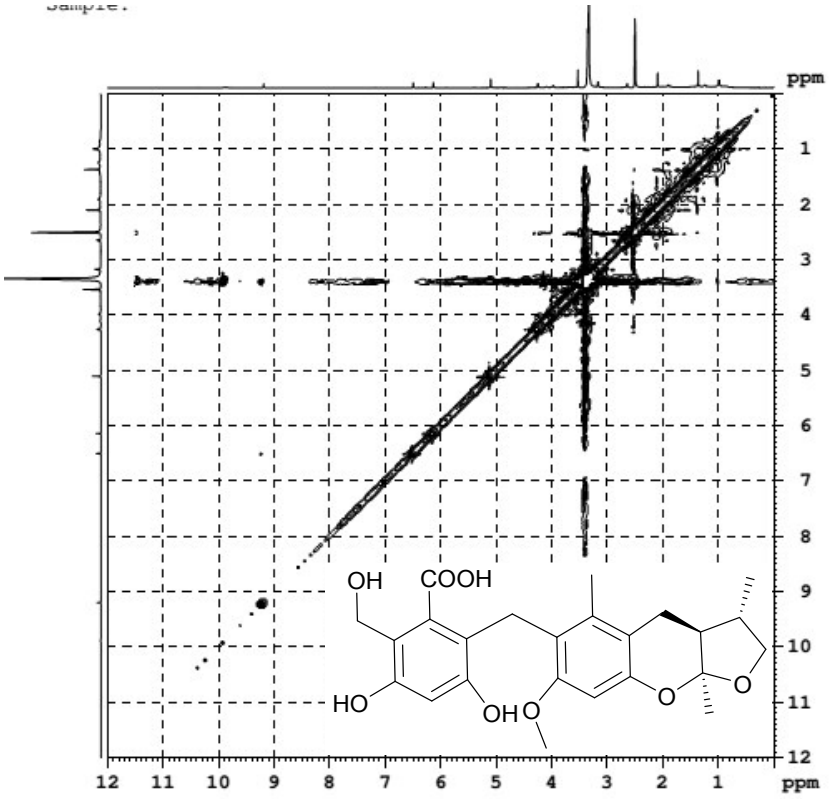

Computational details for ECD of compound **3**

Computational method

The geometry determined from the 1D, 2D NMR and MS analysis of **3** was used as the input for conformational search by CONFLEX. Those conformations whose energy was no more 10 kcal/mol higher than the lowest energy were selected for further optimization by the density functional theory method at the B3LYP/6-31 G* level in Gaussian 09 program package. They were checked by frequency calculation and resulted in no imaginary frequencies. The ECD of the conformer of **3** was then calculated by the TDDFT method at the B3LYP/6-31++G** levels with the CPCM model in methanol solution. The calculated ECD curve was generated using SpecDis 1.51 with $\sigma = 0.16$ ev, and UV shift 0 nm.

Table S7 Energy analysis of **3a**

Label	MMFF	
	rel. E(Kal/mol)	Boltzmann Dist.
3a	0.00	0.529

Table S8 Computational methods for ECD of **3a**

Standard orientation:

Center Number	Atomic Number	Atomic Type	Coordinates (Angstroms) X	Y	Z
1	6	0	0.139383	-1.076020	1.713175
2	6	0	-0.651076	0.017566	1.027194
3	6	0	-0.012146	1.229837	0.699862
4	6	0	1.459298	1.500548	1.019943
5	6	0	2.486334	0.851229	0.087070
6	6	0	3.449143	-0.080232	0.534925
7	6	0	3.565090	-0.398017	1.999750
8	8	0	3.887868	0.685097	2.739328
9	8	0	3.420327	-1.500847	2.493073
10	6	0	4.343492	-0.733583	-0.335845
11	6	0	5.460719	-1.648915	0.123427
12	8	0	5.562741	-2.838656	-0.693546
13	6	0	4.261428	-0.435428	-1.711894
14	8	0	5.080615	-1.037922	-2.618645

15	6	0	3.358420	0.513361	-2.176481
16	6	0	2.496460	1.164481	-1.291562
17	8	0	1.678085	2.089238	-1.858517
18	6	0	-0.786662	2.242384	0.096407
19	8	0	-0.107072	3.402018	-0.225251
20	6	0	-0.830226	4.492297	-0.804952
21	6	0	-2.139140	2.074315	-0.166449
22	6	0	-2.747308	0.856521	0.155822
23	6	0	-2.019281	-0.190658	0.734795
24	6	0	-2.722753	-1.498407	1.042631
25	6	0	-4.084558	-1.620780	0.352638
26	1	0	-4.685731	-2.371054	0.882059
27	6	0	-4.891420	-0.319946	0.343940
28	8	0	-5.900460	-0.512246	-0.608062
29	6	0	-5.455626	-1.465719	-1.601983
30	6	0	-4.074496	-1.979676	-1.149729
31	1	0	-3.293574	-1.388080	-1.643601
32	6	0	-3.839972	-3.459280	-1.454265
33	6	0	-5.514438	0.121937	1.656779
34	8	0	-4.074624	0.774500	-0.170803
35	1	0	0.861362	-1.543773	1.033609
36	1	0	0.713612	-0.680691	2.556930
37	1	0	-0.501915	-1.864943	2.107394
38	1	0	1.615539	2.584561	1.027604
39	1	0	1.658754	1.180948	2.043541
40	1	0	3.935782	0.392625	3.671681
41	1	0	6.432141	-1.158430	-0.004432
42	1	0	5.358013	-1.928484	1.172794
43	1	0	4.736263	-3.339939	-0.585334
44	1	0	5.439263	-1.848755	-2.187688
45	1	0	3.321967	0.756080	-3.233343
46	1	0	1.185237	2.616792	-1.194850
47	1	0	-0.097229	5.285916	-0.952016
48	1	0	-1.268161	4.209664	-1.768230
49	1	0	-1.617152	4.836621	-0.126322
50	1	0	-2.743353	2.848453	-0.621870
51	1	0	-2.101461	-2.349484	0.740930
52	1	0	-2.862034	-1.604981	2.127778
53	1	0	-5.428102	-0.978611	-2.582598
54	1	0	-6.197261	-2.273117	-1.636662
55	1	0	-4.598437	-4.085761	-0.969010
56	1	0	-3.882647	-3.651766	-2.532583
57	1	0	-2.854915	-3.785558	-1.101573
58	1	0	-6.118252	1.019588	1.493842
59	1	0	-6.154388	-0.669009	2.059112
60	1	0	-4.737154	0.354830	2.391037

Table S9 2D Structures of **3a** and **3b**

label	structure
3a	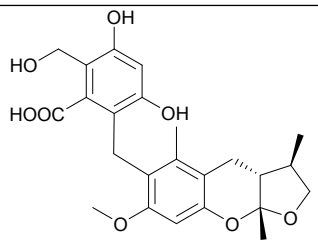
3b	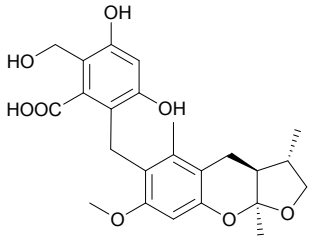

Figure S31. B3LYP/6-31 G* optimized lowest energy 3D conformer of **3**

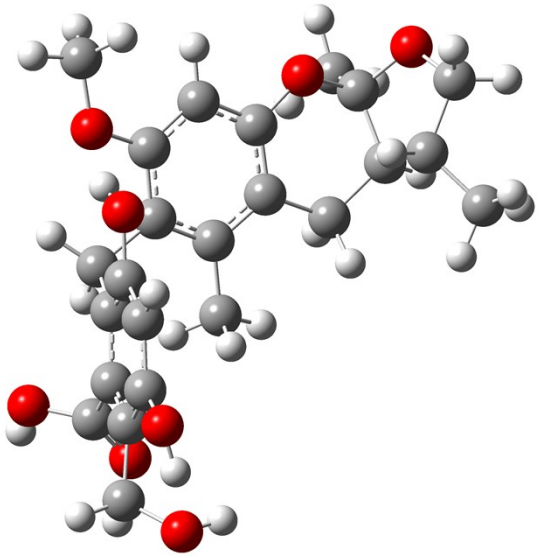

Figure S32. Experimental and suitable calculated ECD spectra of **3**

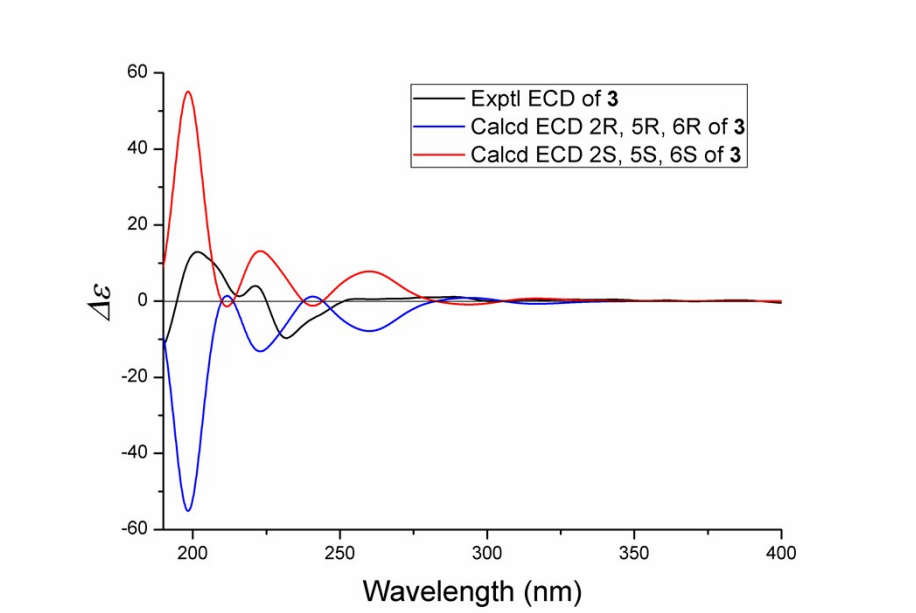

8. The spectra of Phomeketale D (4)

Figure S33. The UV spectrum of compound **4**

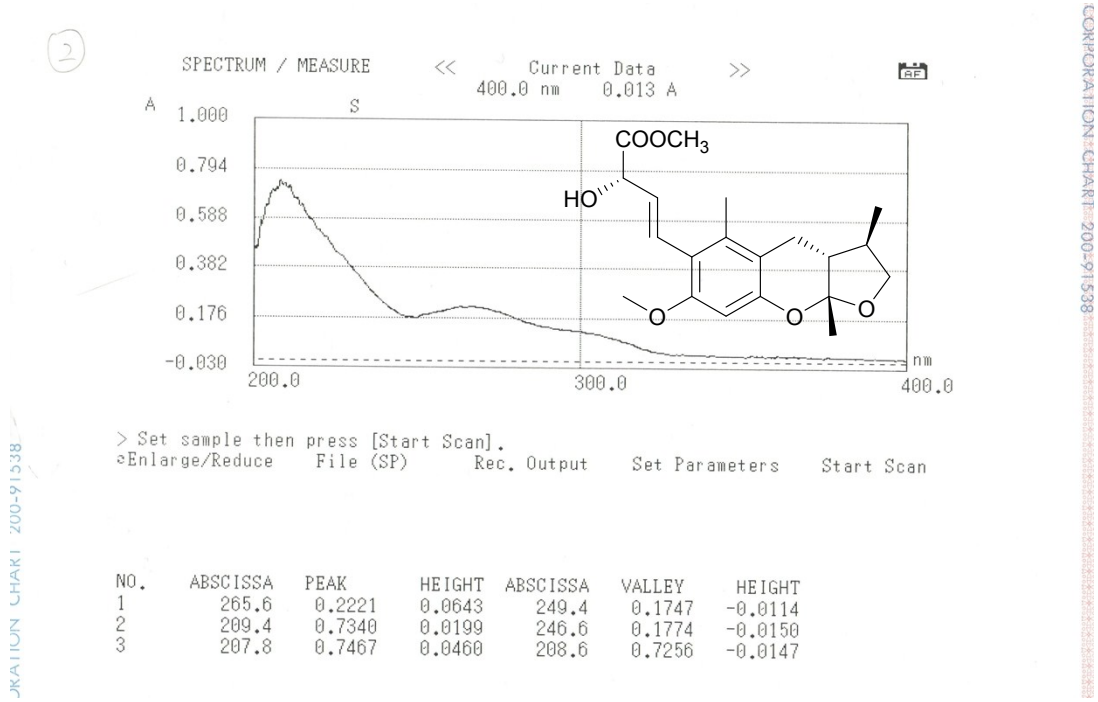

Figure S34. The IR spectrum of compound **4**

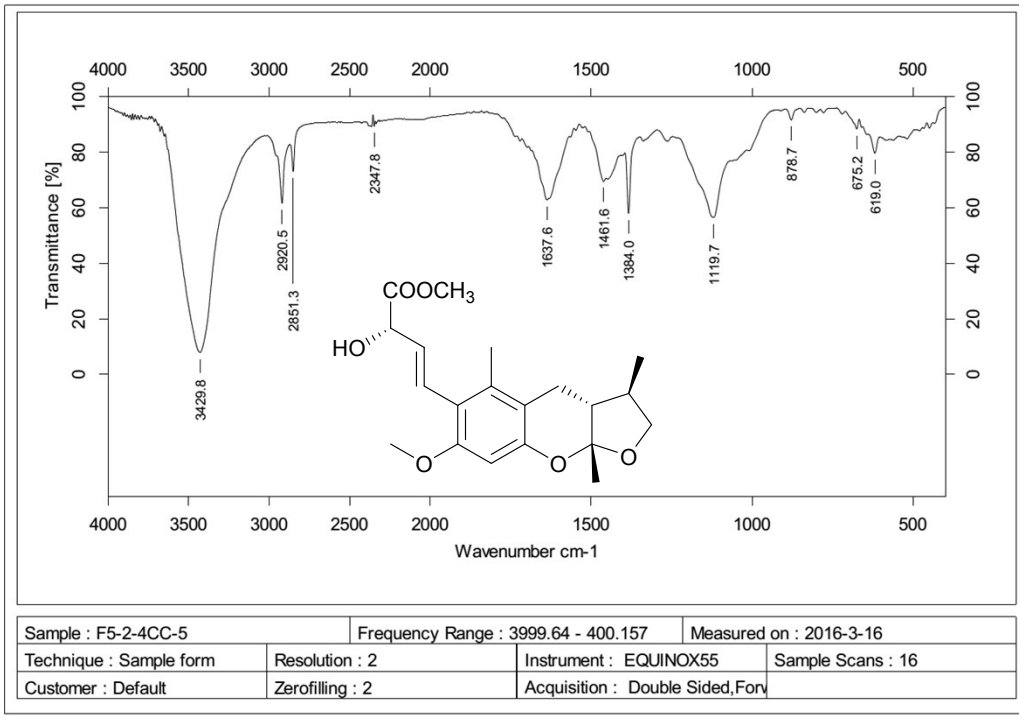

Sample : F5-2-4CC-5	Frequency Range : 3999.64 - 400.157	Measured on : 2016-3-16	
Technique : Sample form	Resolution : 2	Instrument : EQUINOX55	Sample Scans : 16
Customer : Default	Zerofilling : 2	Acquisition : Double Sided,For	

Figure S35. The HR-ESI-MS spectrum of compound **4**

Mass Spectrum Molecular Formula Report

Analysis Info

Analysis Name	D:\Data\20160318CEYANG\F5-2-4CC-5_1-C,1_01_6732.d	Acquisition Date	3/18/2016 12:40:09 PM
Method	20131026_ceyang.m	Operator	Bruker Customer
Sample Name	F5-2-4CC-5	Instrument / Ser#	micrOTOF-Q 125
Comment			

Acquisition Parameter

Source Type	ESI	Ion Polarity	Positive	Set Nebulizer	1.2 Bar
Focus	Active	Set Capillary	4500 V	Set Dry Heater	180 °C
Scan Begin	50 m/z	Set End Plate Offset	-500 V	Set Dry Gas	8.0 l/min
Scan End	3000 m/z	Set Collision Cell RF	400.0 Vpp	Set Divert Valve	Source

Generate Molecular Formula Parameter

Formula, min.	C20H26O6Na						
Formula, max.							
Measured m/z	385.163	Tolerance	5	ppm	Charge	1	
Check Valence	no	Minimum	0		Maximum	0	
Nirogen Rule	no	Electron Configuration	both				
Filter H/C Ratio	no	Minimum	0		Maximum	3	
Estimate Carbon	yes						

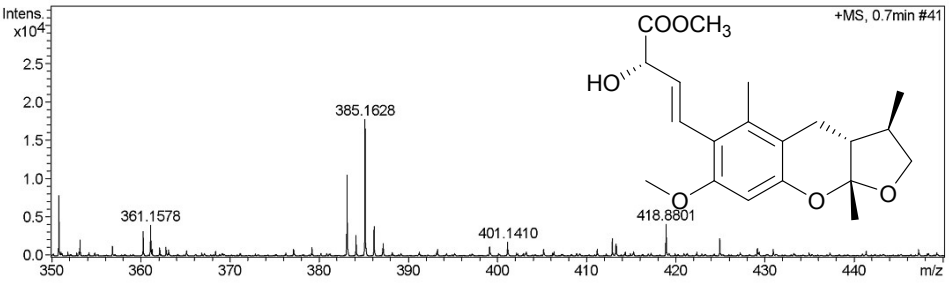

Sum Formula	Sigma	m/z	Err [ppm]	Mean Err [ppm]	Err [mDa]	rdb	N Rule	e⁻
C 20 H 26 Na 1 O 6	0.028	385.1622	-1.56	-5.55	-0.60	7.50	ok	even

Figure S36. The ^{1}H-NMR spectrum of compound **4**

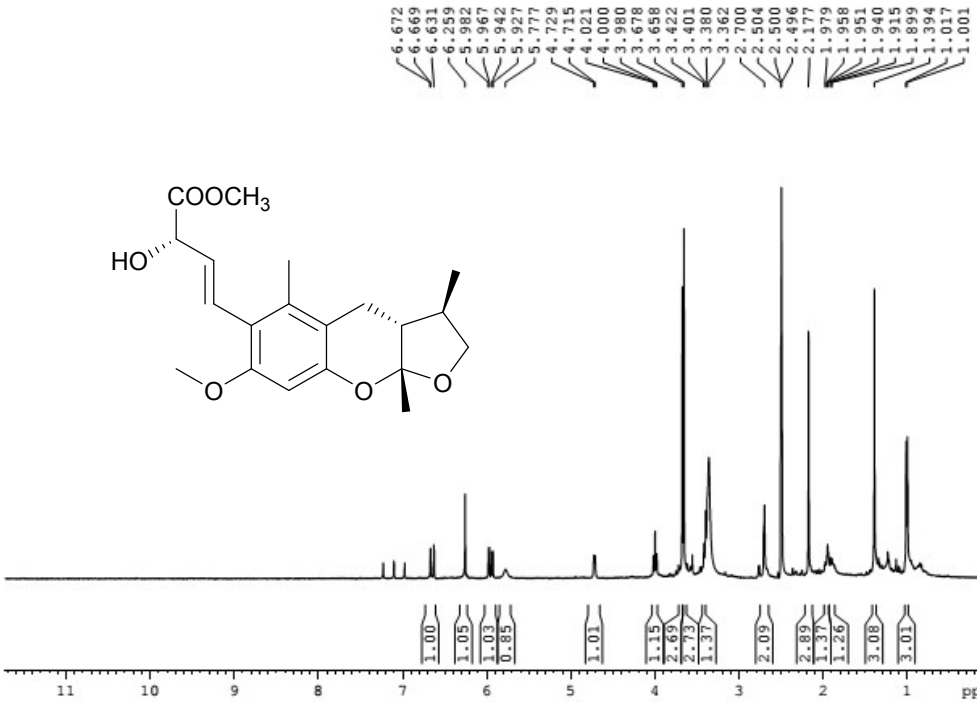

Figure S37. The ^{13}C-NMR spectrum of compound **4**

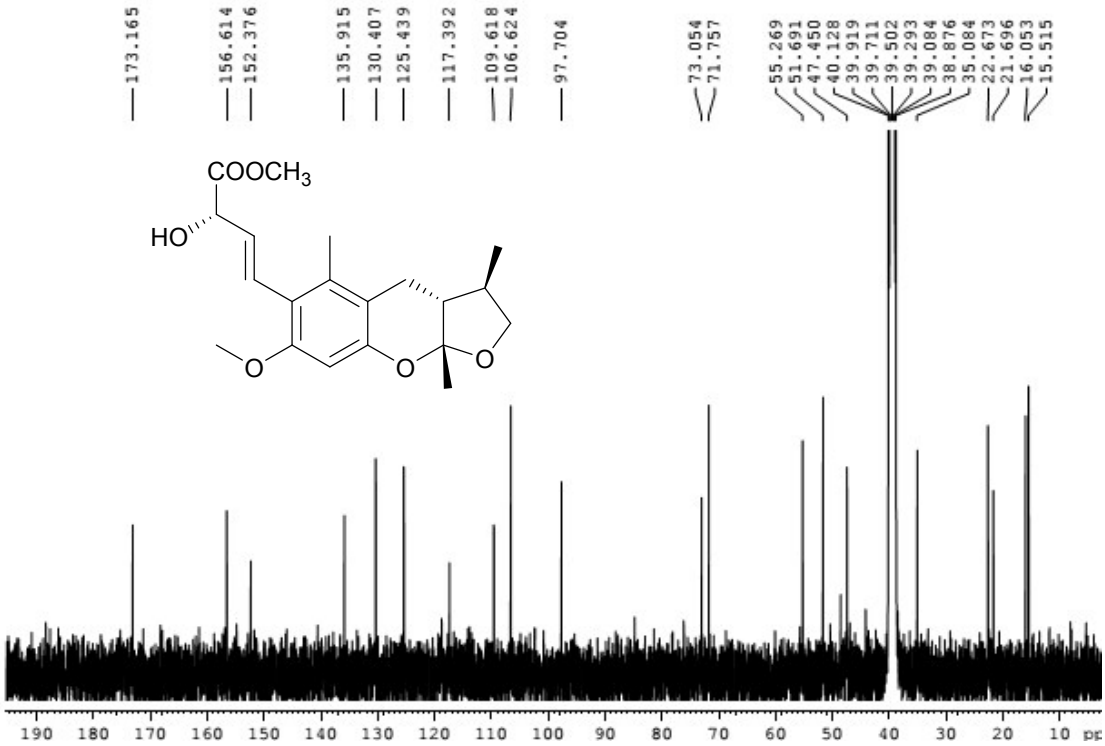

Figure S38. The HSQC spectrum of compound **4**

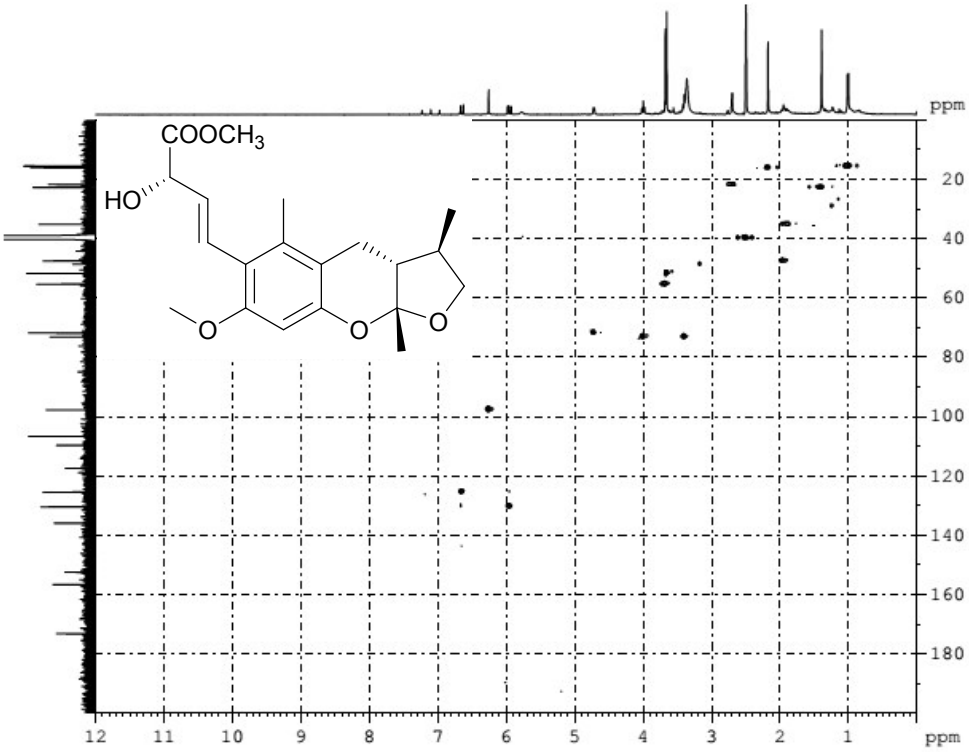

Figure S39. The HMBC spectrum of compound **4**

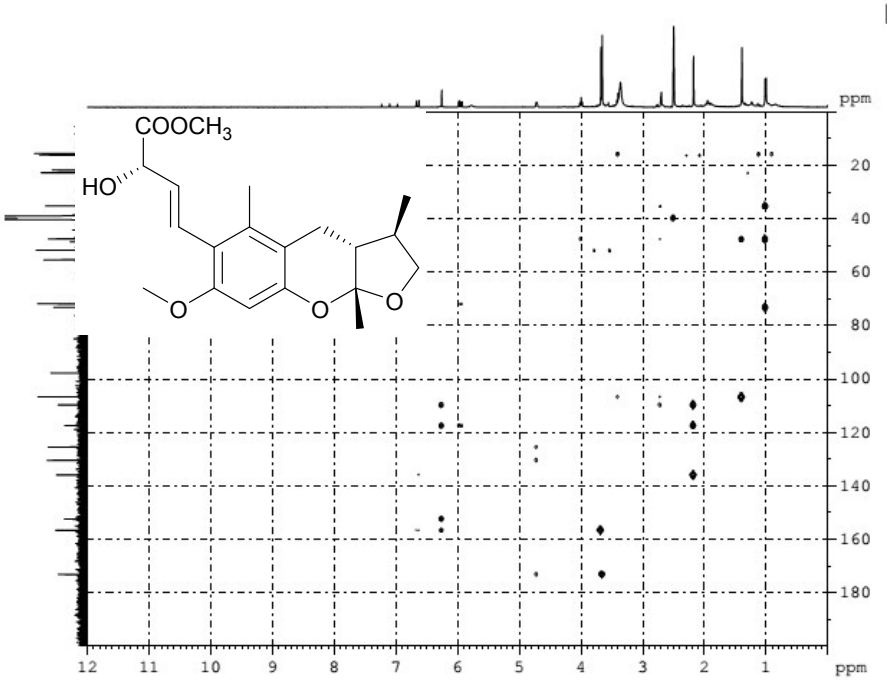

Figure S40. The NOESY spectrum of compound **4**

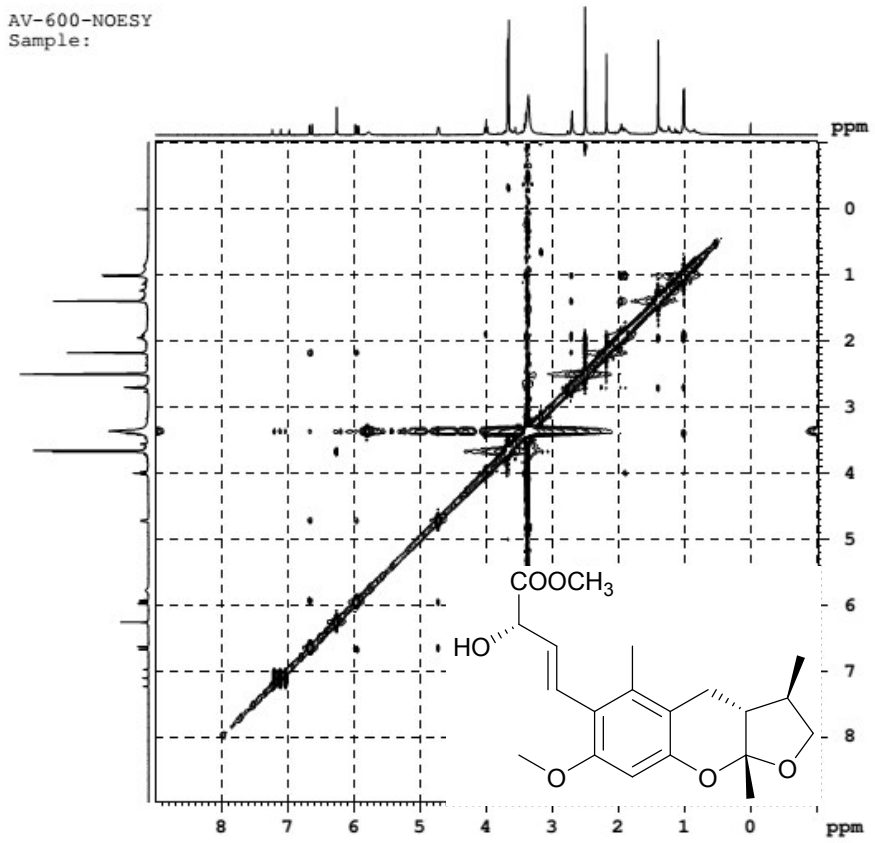

Computational details for ECD of compound **4**

Computational method

The geometry determined from the 1D, 2D NMR and MS analysis and via confirmed the CD data of the in situ formed [$Rh_2(OCOCF_3)_4$] complex method analysis of **4** was used as the input for conformational search by CONFLEX. Those conformations whose energy was no more 10 kcal/mol higher than the lowest energy were selected for further optimization by the density functional theory method at the B3LYP/6-31 G* level in Gaussian 09 program package. They were checked by frequency calculation and resulted in no imaginary frequencies. The ECD of the conformer of **4** was then calculated by the TDDFT method at the B3LYP/6-31++G** levels with the CPCM model in methanol solution. The calculated ECD curve was generated using SpecDis 1.51 with σ = 0.16 ev, and UV shift -18 nm

Table S10 Energy analysis of **4a**

Label	MMFF	
	rel. E(Kal/mol)	Boltzmann Dist.
4a	0.00	0.186

Table S11 Computational methods for ECD of **4a**

Standard orientation:

Center Number	Atomic Number	Atomic Type	Coordinates (Angstroms) X	Y	Z
1	6	0	-1.405677	-3.387319	-0.084307
2	8	0	-1.613506	-2.003769	0.186965
3	6	0	-0.529634	-1.182678	0.298737
4	6	0	0.772793	-1.659364	0.202856
5	6	0	1.849006	-0.772954	0.305250
6	8	0	3.081361	-1.352187	0.169767
7	6	0	4.288151	-0.605982	0.510608
8	8	0	5.296472	-1.134051	-0.306121
9	6	0	5.340593	-0.405795	-1.555954
10	6	0	4.323919	0.747420	-1.444514
11	1	0	3.371711	0.428680	-1.886514
12	6	0	4.779842	2.035289	-2.130377
13	6	0	4.624437	-0.878360	1.966710
14	6	0	4.141961	0.856851	0.085327
15	1	0	5.002578	1.400451	0.495777
16	6	0	2.853244	1.518572	0.583157
17	6	0	1.648632	0.599383	0.504773
18	6	0	0.324604	1.069922	0.631958
19	6	0	0.093454	2.543881	0.913917
20	6	0	-0.789990	0.198627	0.516311
21	6	0	-2.147729	0.759097	0.579983
22	6	0	-3.331769	0.150744	0.765187
23	6	0	-4.642901	0.917988	0.793321
24	1	0	-5.188618	0.659579	1.712447
25	6	0	-5.503793	0.473909	-0.395480
26	8	0	-5.922522	-0.786449	-0.284673
27	6	0	-6.691527	-1.306096	-1.393872
28	8	0	-5.738915	1.208043	-1.338967
29	8	0	-4.497175	2.322008	0.742885
30	1	0	-0.851566	-3.875267	0.726188
31	1	0	-2.401681	-3.826391	-0.157886

32	1	0	-0.870625	-3.533074	-1.030037
33	1	0	0.990868	-2.707982	0.047258
34	1	0	5.117447	-1.090749	-2.380982
35	1	0	6.364650	-0.033436	-1.681986
36	1	0	5.726213	2.393499	-1.706688
37	1	0	4.929425	1.877826	-3.204806
38	1	0	4.034823	2.830865	-2.015912
39	1	0	3.812438	-0.539992	2.617634
40	1	0	4.765192	-1.952853	2.116913
41	1	0	5.543747	-0.356458	2.248659
42	1	0	2.680728	2.429211	-0.001711
43	1	0	3.004087	1.857189	1.618063
44	1	0	-0.636531	2.687710	1.716152
45	1	0	1.010018	3.048478	1.220948
46	1	0	-0.289148	3.073758	0.031231
47	1	0	-2.203253	1.837650	0.471368
48	1	0	-3.422836	-0.918988	0.903432
49	1	0	-6.938523	-2.330461	-1.119123
50	1	0	-7.599183	-0.714830	-1.531904
51	1	0	-6.094442	-1.285596	-2.308077
52	1	0	-4.688943	2.573616	-0.180841

Table S12 2D Structures of **4a** and **4b**

label	structure
4a	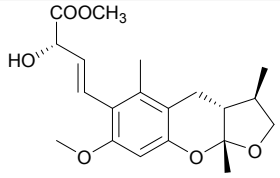
4b	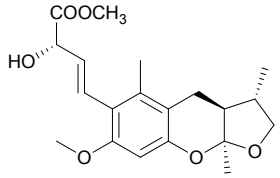

Figure S41. B3LYP/6-31 G* optimized lowest energy 3D conformer of **4**

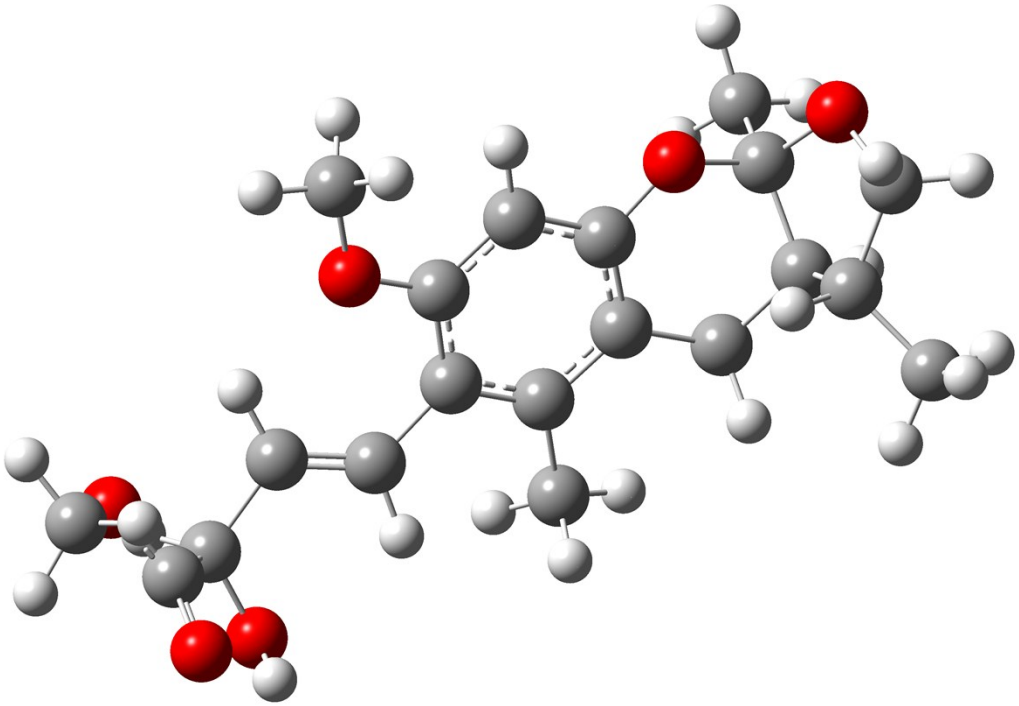

Figure S42. Experimental and suitable calculated ECD spectra of **4**

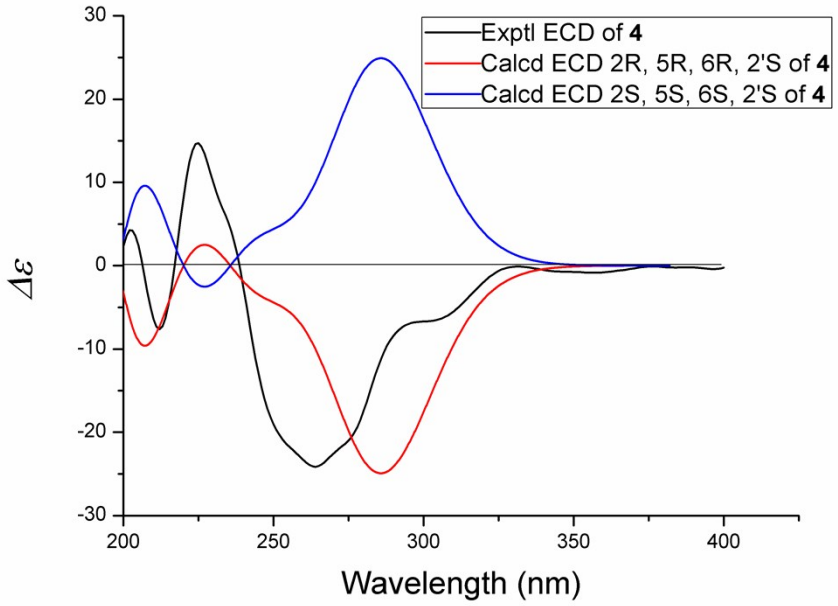

Figure S43. The CD spectrum of compound **4** in a $CDCl_3$ of $[Rh_2(OCOCF_3)_4]$ (the inherent contribution of compound **4** was subtracted)

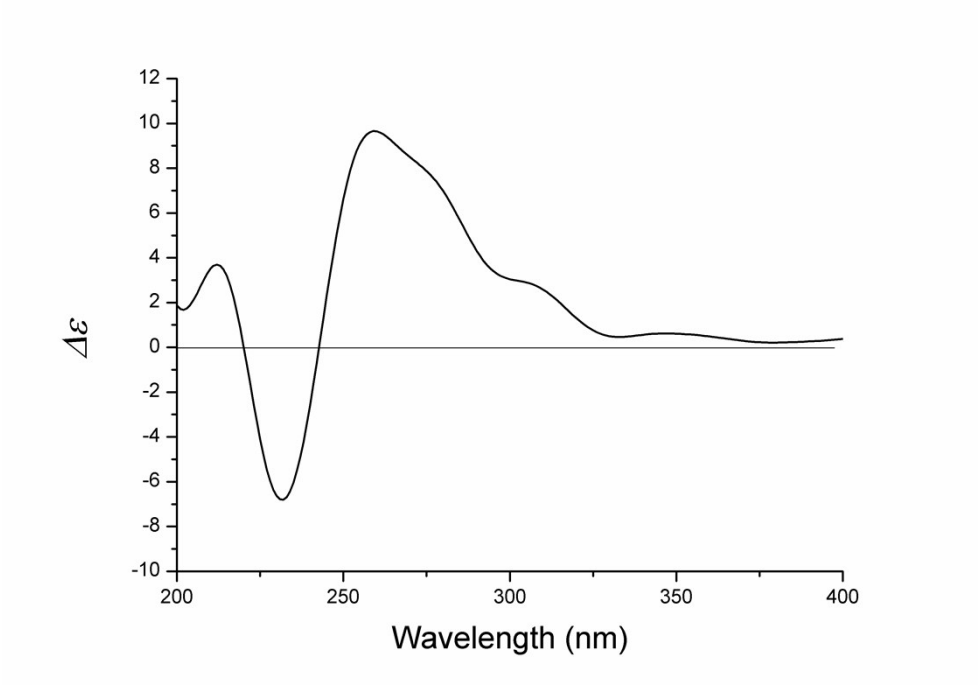

9. The spectra of Phomeketale E (5)

Figure S44. The UV spectrum of compound **5**

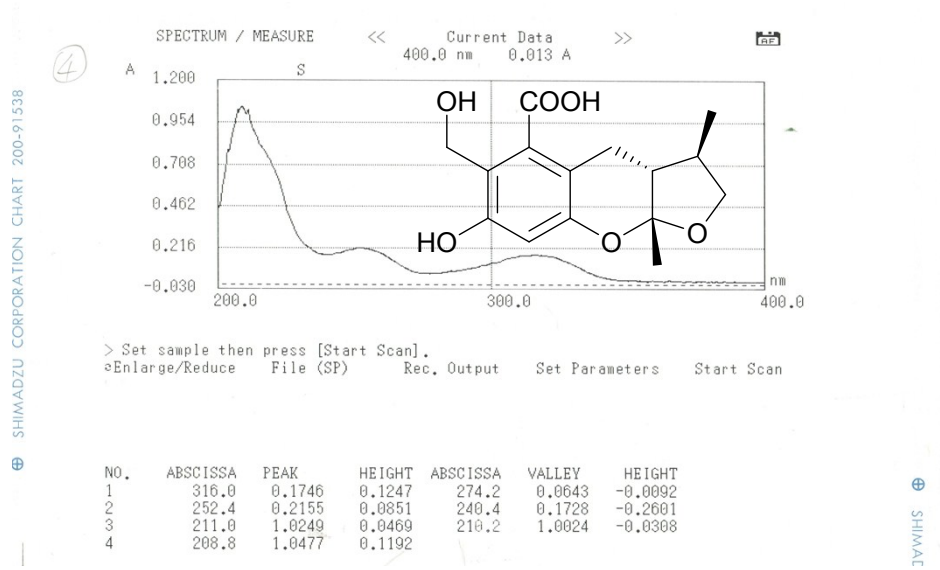

Figure S45. The IR spectrum of compound **5**

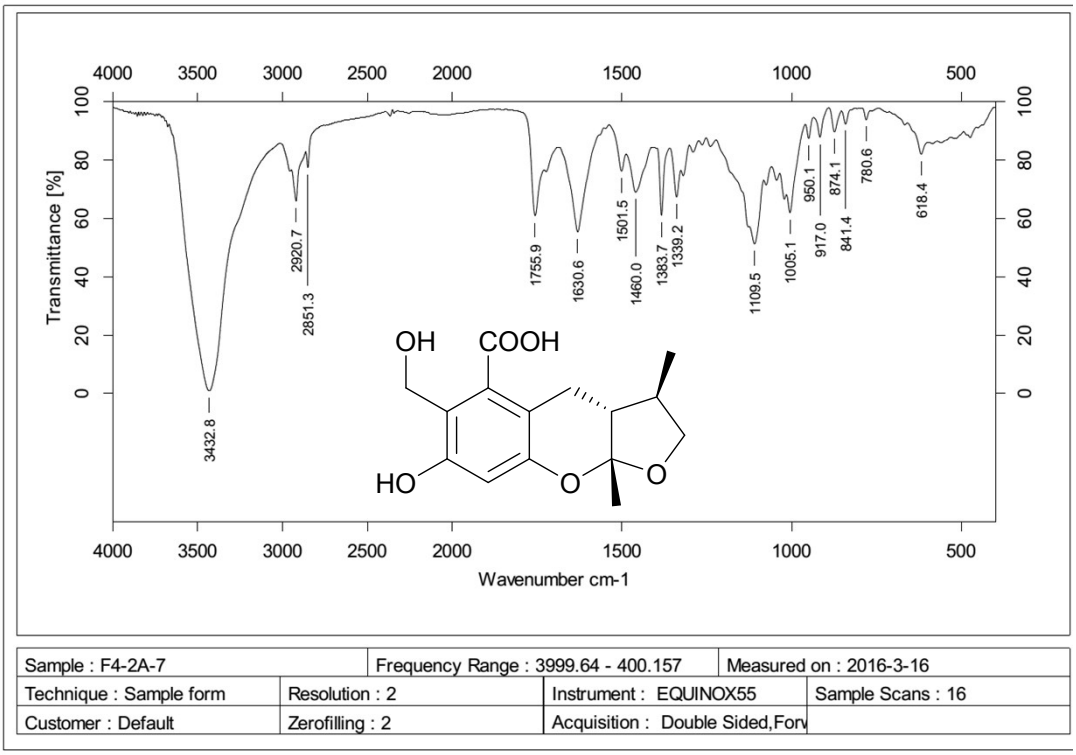

Figure S46. The HR-ESI-MS spectrum of compound **5**

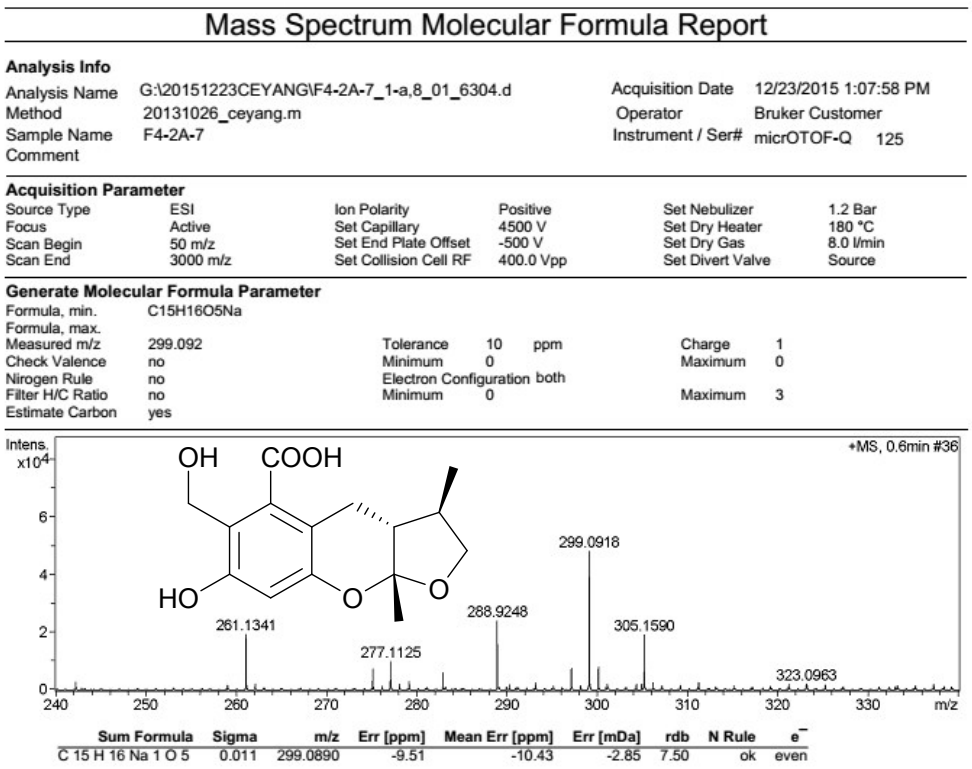

Figure S47. The [1]H-NMR spectrum of compound **5**

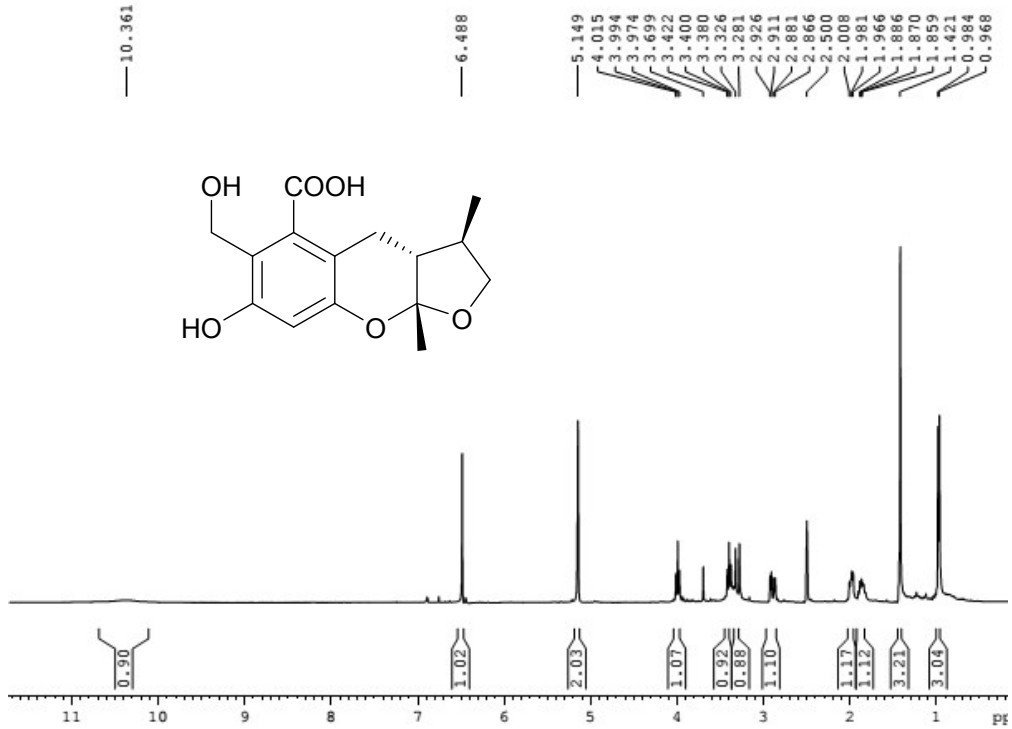

Figure S48. The [13]C-NMR spectrum of compound **5**

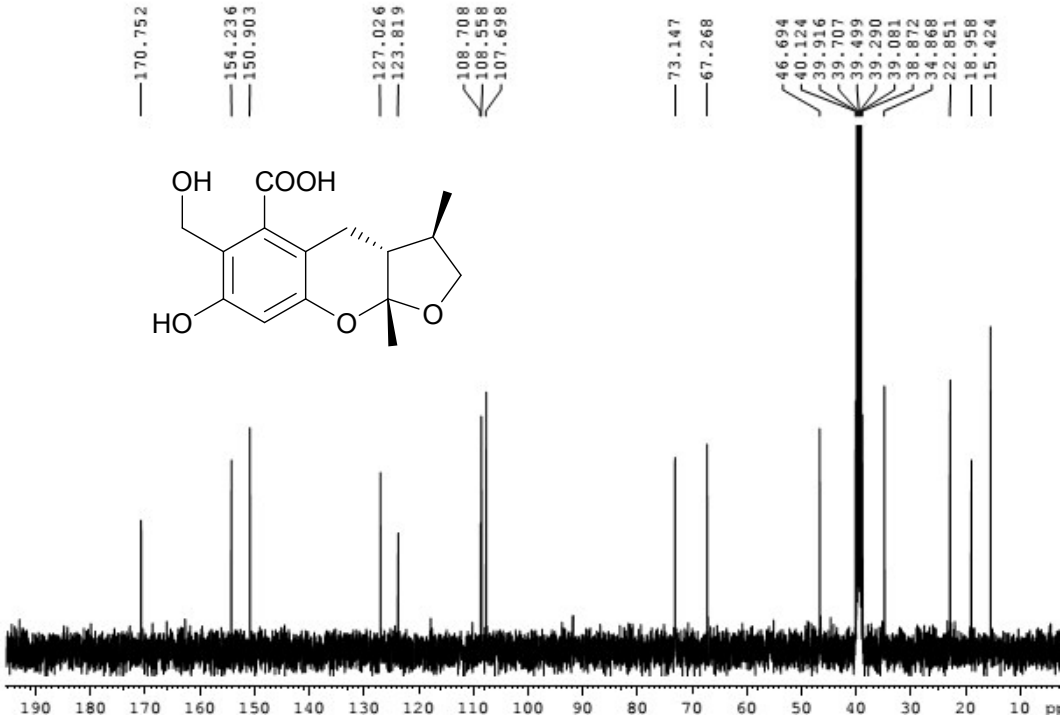

Figure S49. The HSQC spectrum of compound **5**

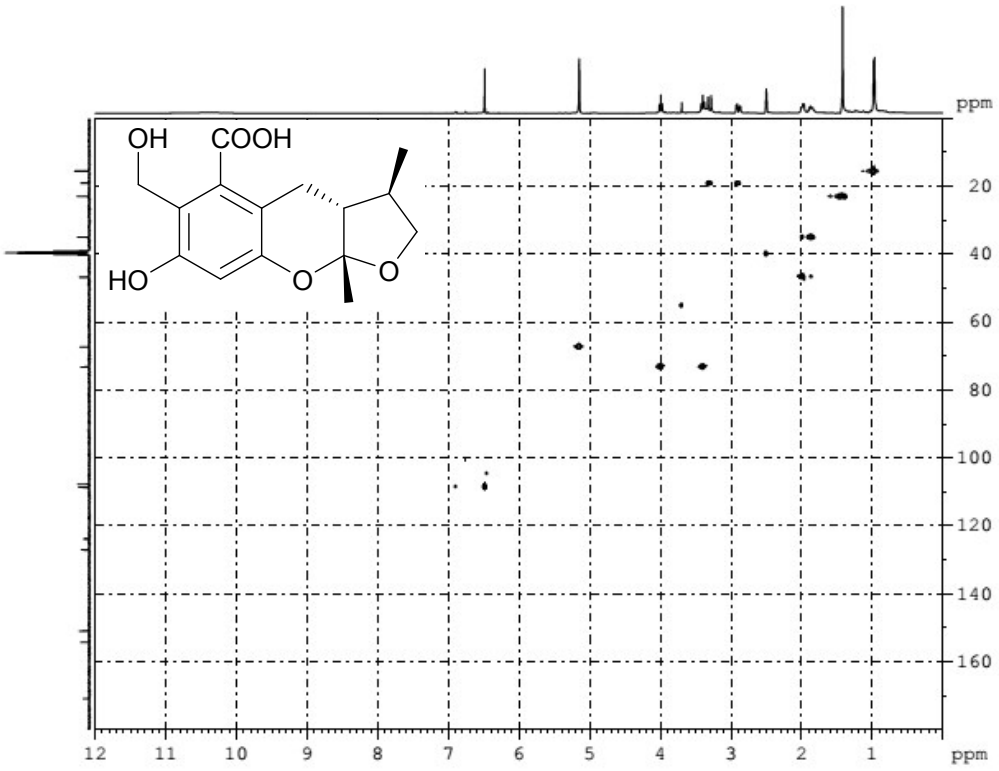

Figure S50. The HMBC spectrum of compound **5**

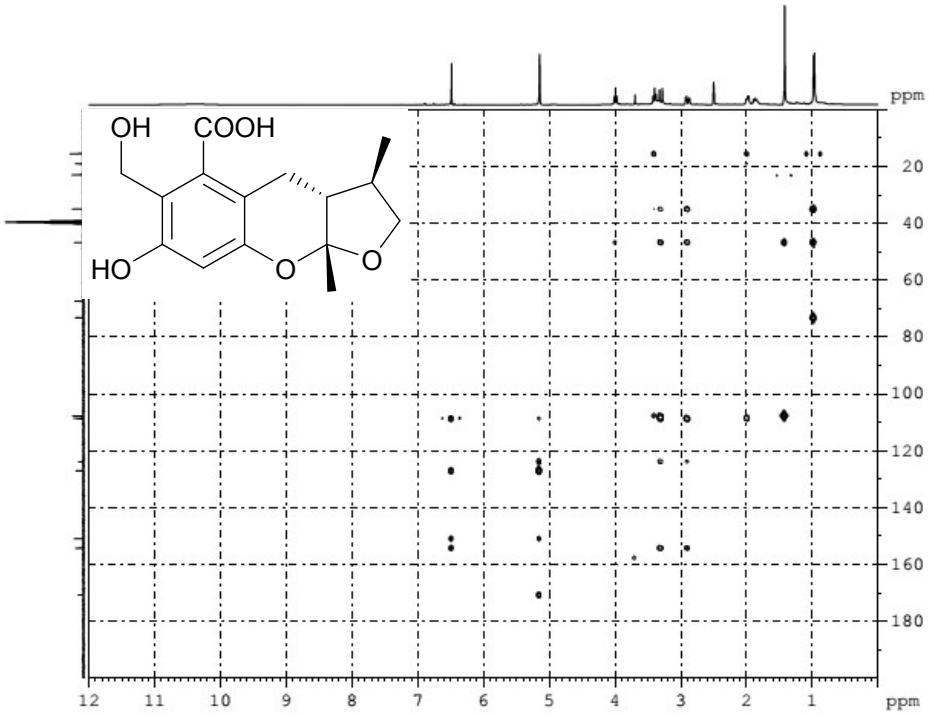

Figure S51. The NOESY spectrum of compound **5**

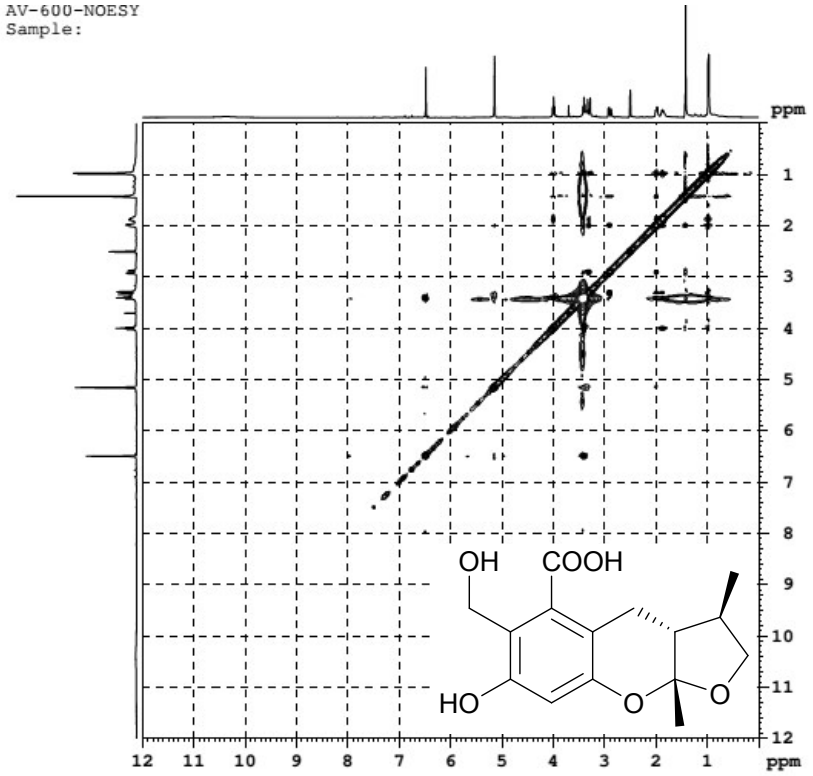

Figure S52. The ^{1}H-^{1}H COSY spectrum of compound **5**

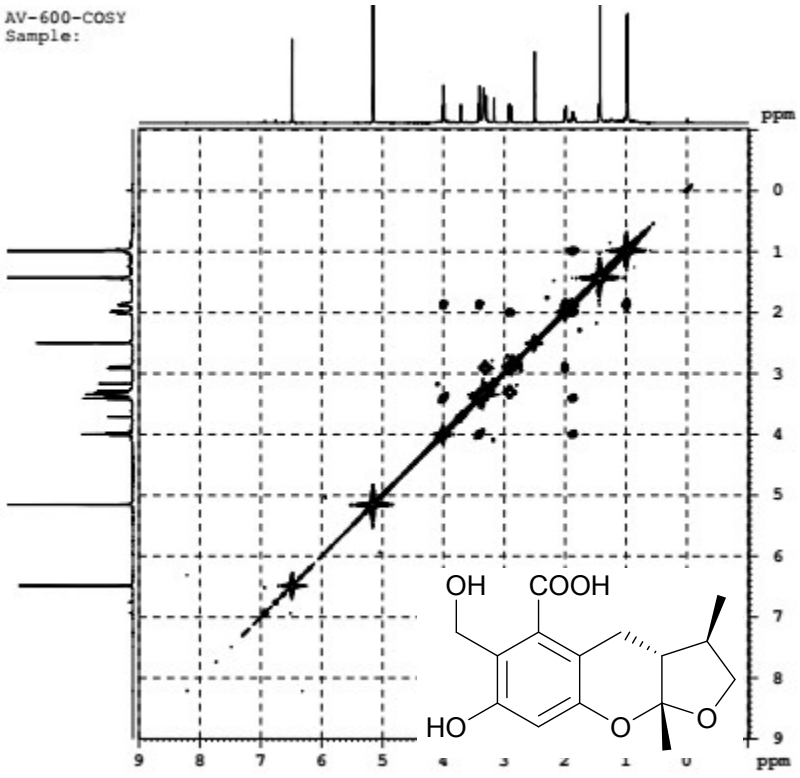

Figure S53. The DEPT-135 spectrum of compound **5**

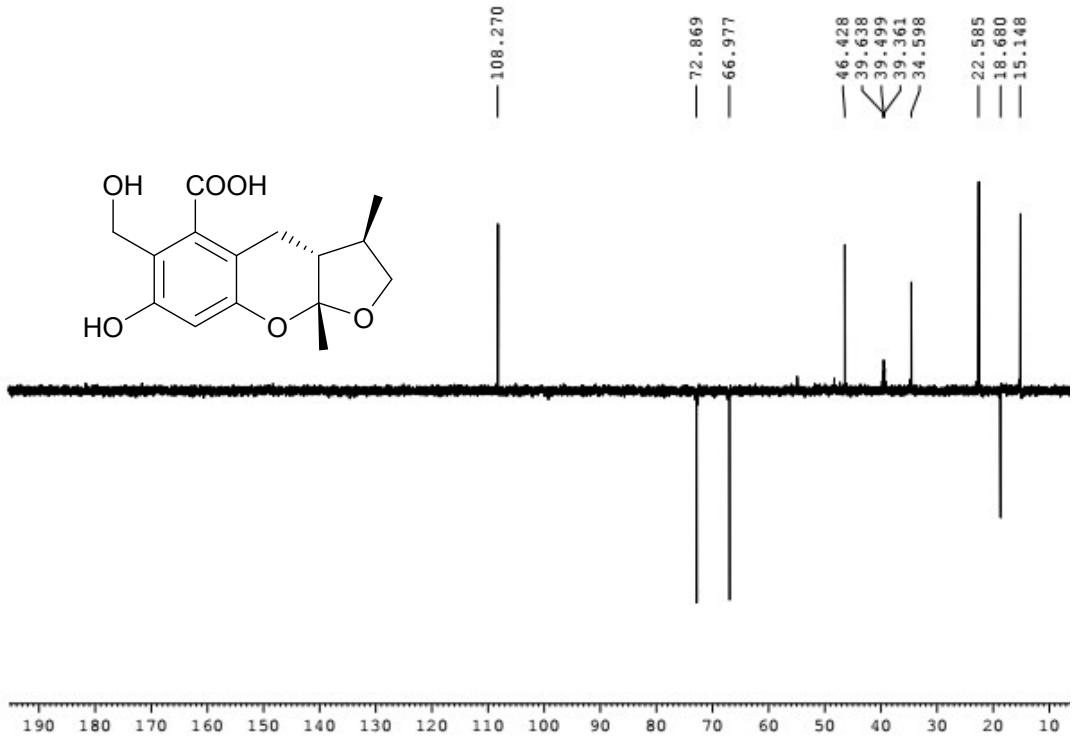

Computational details for ECD of compound **5**

Computational method

The Spartan 14.0 (Wavefunction Inc., Irvine, CA, USA) searches using molecular mechanics MMFF were performed for **5a**, which gave 6 conformers. The only low-energy conformer of **5a** accounting for more than 30% Boltzmann distribution was further optimized and analysed frequency in Gaussian 09 program package, using the density functional theory (DFT) at the B3LYP/6-31G (d, p) level and the same way in the methanol, resulted in no imaginary frequencies. Solvent effects were taken into consideration by using the conductor polarizable continuum model (CPCM). The conformer of **5a** was calculated electronic circular dichroism (ECD) by the time-dependent density functional theory (TD-DFT) method at the B3LYP/6-31G (d, p) level with the CPCM model in methanol solution. The calculated ECD curve of the **5a** was generated using SpecDis 1.51 with $\sigma = 0.16$ eV at 0 nm shift.

Table S13 Energy analysis of **5a**

Label	MMFF	
	rel. E(Kal/mol)	Boltzmann Dist.
5a	0.00	0.632

Table S14 Computational methods for ECD of **5a**

Standard orientation:

Center Number	Atomic Number	Atomic Type	Coordinates (Angstroms) X	Y	Z
1	6	0	-4.099842	1.792412	0.736617
2	8	0	-4.074017	0.508829	0.260482
3	6	0	-2.923437	-0.211666	0.191032
4	6	0	-1.746502	0.313158	0.612694
5	6	0	-1.703866	1.670785	1.160409
6	6	0	-2.972572	2.406424	1.180497
7	6	0	-3.166149	-1.597175	-0.383933
8	6	0	-1.867436	-2.446972	-0.395686
9	6	0	-0.656065	-2.021584	0.418084
10	6	0	-0.496489	-0.498043	0.615767
11	6	0	0.656041	-2.021608	-0.418146
12	6	0	0.496502	-0.498064	-0.615837
13	6	0	1.867424	-2.447083	0.395538
14	6	0	3.166099	-1.597222	0.383994
15	6	0	2.923437	-0.211726	-0.191008
16	6	0	1.746534	0.313107	-0.612749
17	8	0	4.074035	0.508751	-0.260418
18	6	0	4.099909	1.792312	-0.736603
19	6	0	2.972673	2.406331	-1.180562
20	6	0	1.703953	1.670716	-1.160514
21	8	0	-0.652321	2.165609	1.599752
22	8	0	0.652443	2.165541	-1.599938
23	6	0	2.920413	3.809272	-1.721950
24	6	0	5.498482	2.322636	-0.672444
25	6	0	-2.920263	3.809384	1.721832
26	6	0	-5.498408	2.322760	0.672508
27	6	0	-4.170513	-2.372540	0.514159
28	6	0	-3.670715	-1.525009	-1.867090
29	6	0	4.170661	-2.372544	-0.513915
30	6	0	3.670428	-1.525045	1.867234
31	6	0	5.106613	-1.051843	2.117625
32	8	0	-1.837042	-3.492327	-1.022207
33	8	0	1.837070	-3.492558	1.021865
34	6	0	-5.107012	-1.052029	-2.117262

35	1	0	-0.635456	-2.639840	1.323264
36	1	0	0.067104	-0.274177	1.526653
37	1	0	0.635343	-2.639871	-1.323319
38	1	0	-0.067091	-0.274191	-1.526721
39	1	0	3.887774	4.312704	-1.703752
40	1	0	2.552503	3.802080	-2.754378
41	1	0	2.208345	4.409084	-1.143590
42	1	0	5.840499	2.364267	0.368576
43	1	0	6.177609	1.654327	-1.213735
44	1	0	5.576807	3.320295	-1.102252
45	1	0	-2.208341	4.409216	1.143311
46	1	0	-3.887650	4.312772	1.703815
47	1	0	-2.552143	3.802234	2.754184
48	1	0	-5.840436	2.364463	-0.368506
49	1	0	-6.177538	1.654426	1.213763
50	1	0	-5.576712	3.320394	1.102378
51	1	0	-4.376862	-3.351059	0.071160
52	1	0	-5.108301	-1.821416	0.609700
53	1	0	-3.762153	-2.524762	1.518933
54	1	0	-2.975767	-0.890421	-2.432097
55	1	0	-3.560014	-2.538138	-2.264144
56	1	0	5.108447	-1.821389	-0.609289
57	1	0	4.376955	-3.351053	-0.070872
58	1	0	3.762484	-2.524784	-1.518760
59	1	0	2.975310	-0.890585	2.432172
60	1	0	3.559828	-2.538209	2.264226
61	1	0	5.318252	-1.118005	3.191076
62	1	0	5.840269	-1.680446	1.602278
63	1	0	5.268891	-0.017173	1.807819
64	1	0	-5.318803	-1.118219	-3.190682
65	1	0	-5.840490	-1.680752	-1.601811
66	1	0	-5.269409	-0.017387	-1.807428

Table S15 2D Structures of **5a**

label	structure
5a	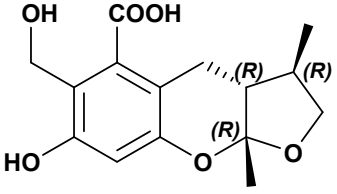
5b	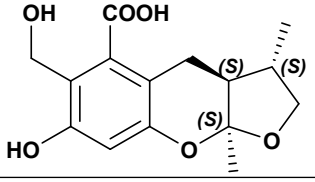

Figure S54. B3LYP/6-31 G* optimized lowest energy 3D conformer of **5**

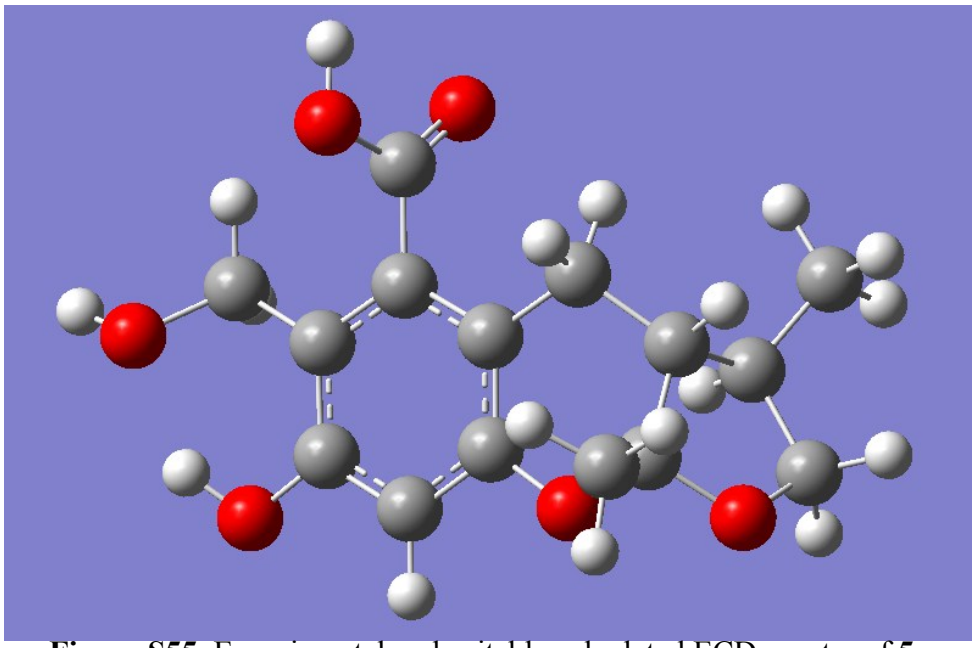

Figure S55. Experimental and suitable calculated ECD spectra of **5**

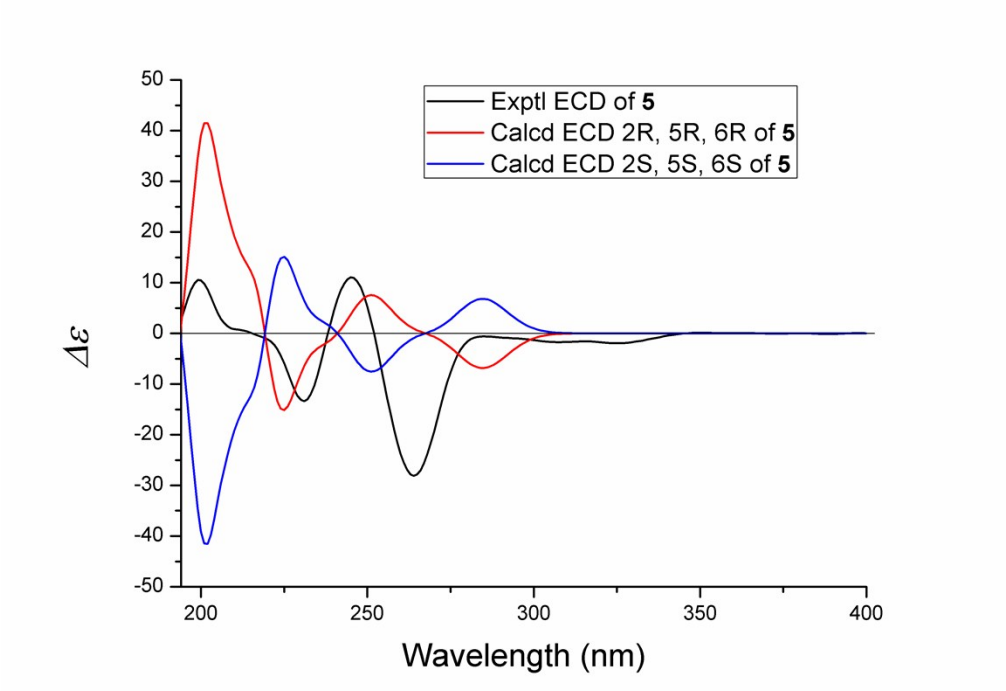

10. The spectra of Phomeketale F (6)

Figure S56. The UV spectrum of compound **6**

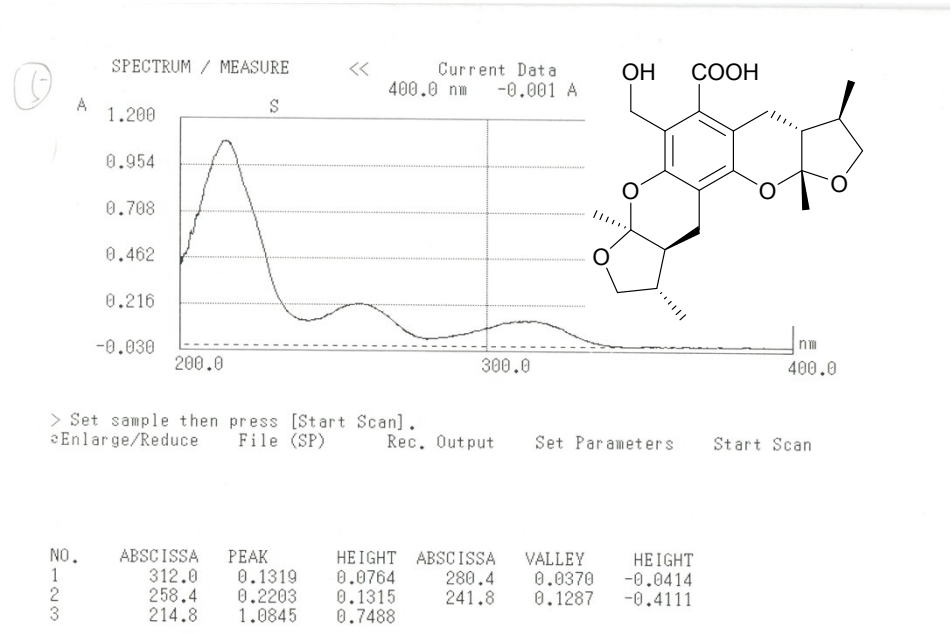

NO.	ABSCISSA	PEAK	HEIGHT	ABSCISSA	VALLEY	HEIGHT
1	312.0	0.1319	0.0764	280.4	0.0370	-0.0414
2	258.4	0.2203	0.1315	241.8	0.1287	-0.4111
3	214.8	1.0845	0.7488			

Figure S57. The IR spectrum of compound **6**

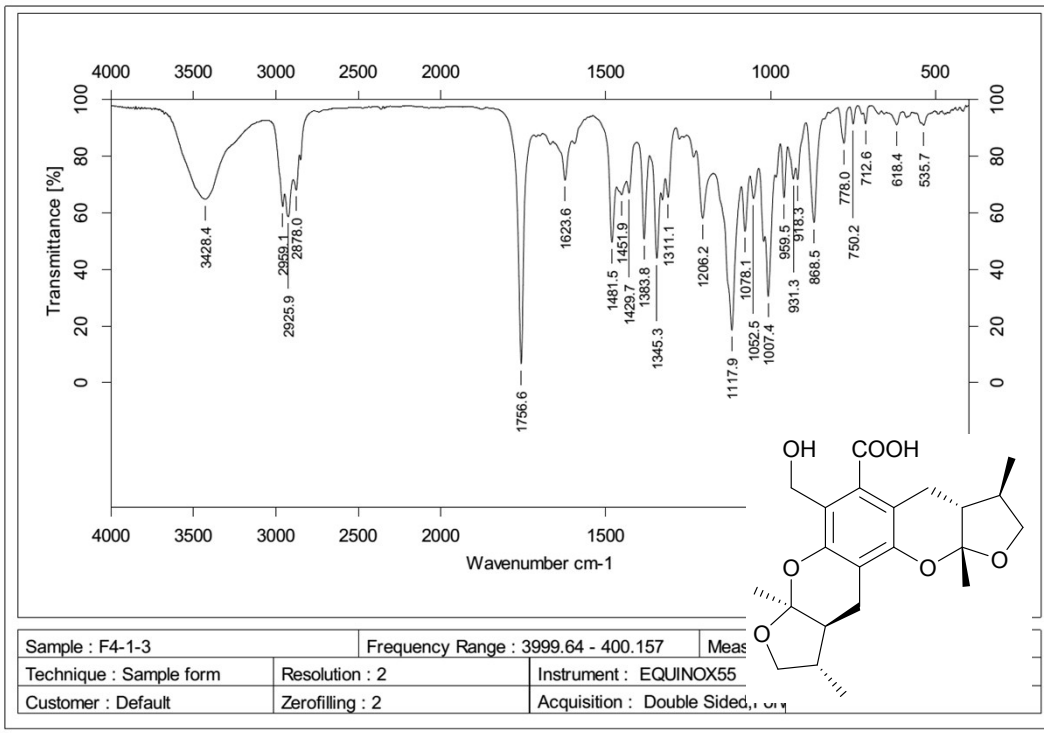

Figure S58. The HR-ESI-MS spectrum of compound **6**

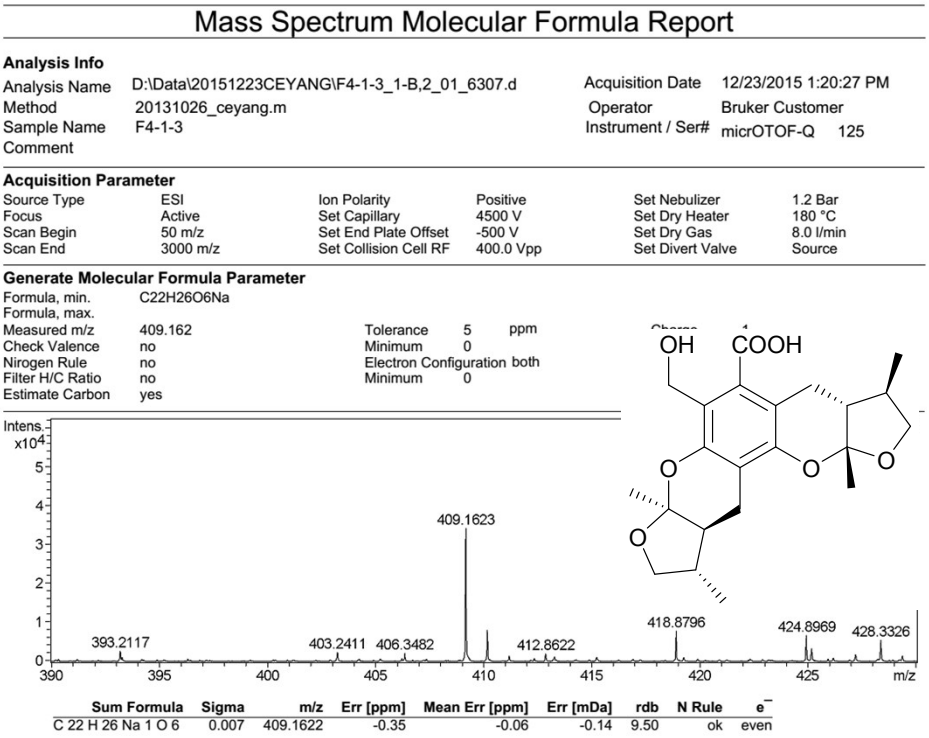

Figure S59. The ^{1}H-NMR spectrum of compound **6**

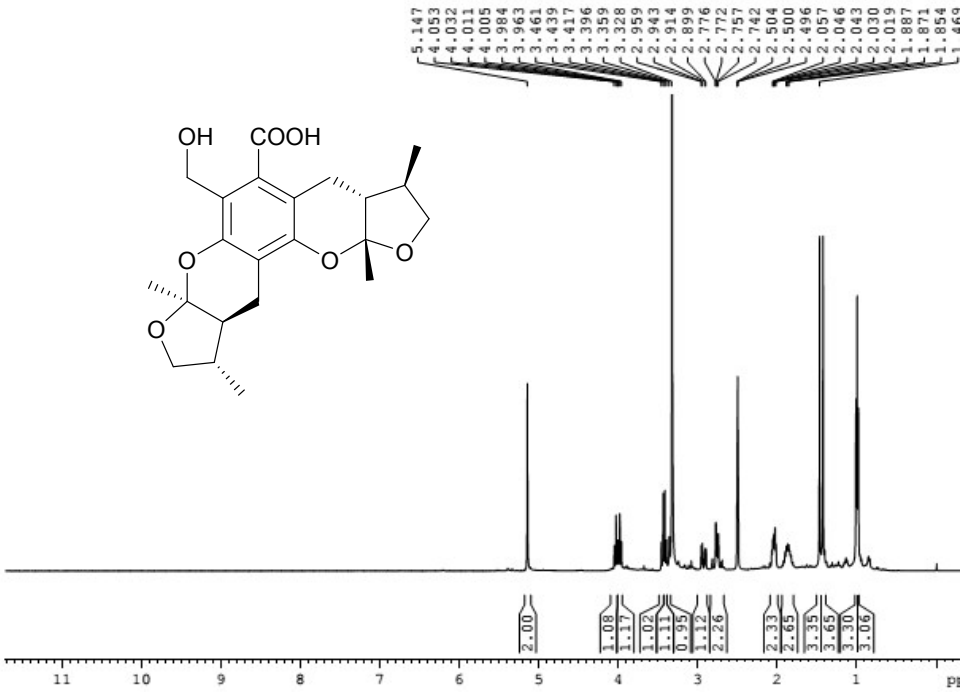

Figure S60. The ^{13}C-NMR spectrum of compound **6**

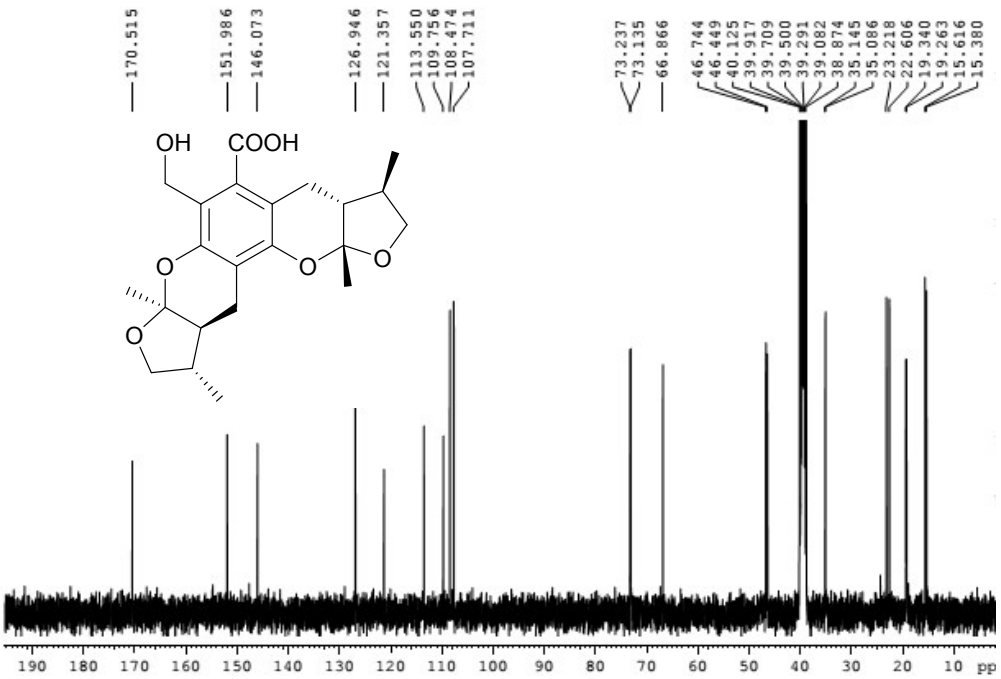

Figure S61. The HSQC spectrum of compound **6**

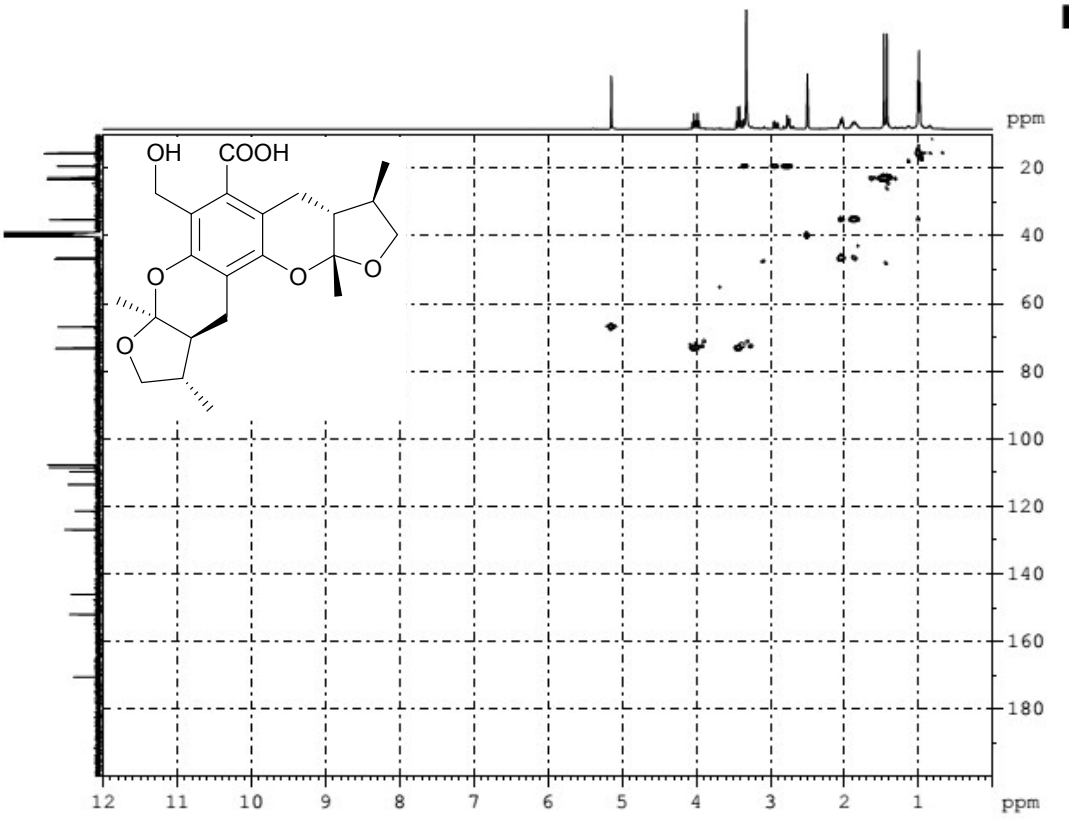

Figure S62. The HMBC spectrum of compound **6**

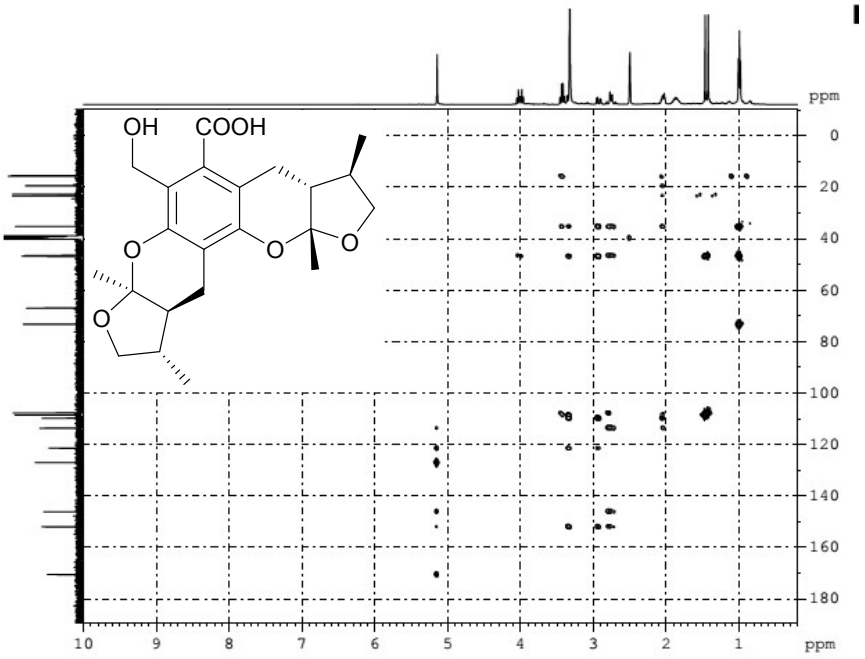

Figure S63. The NOESY spectrum of compound **6**

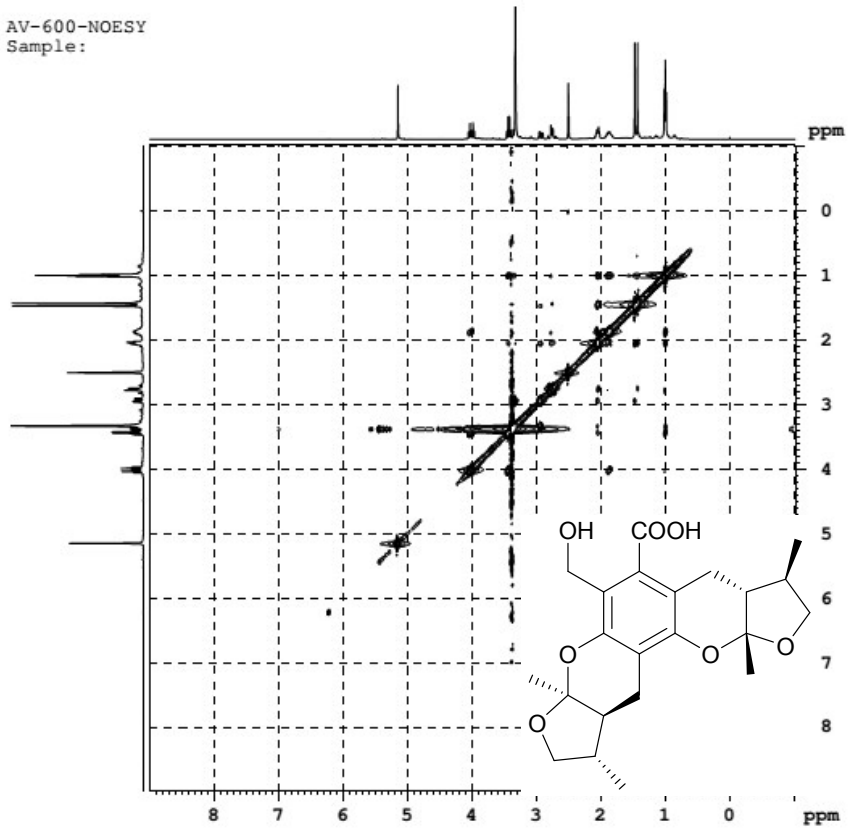

Figure S64. The ^{1}H-^{1}H COSY spectrum of compound **6**

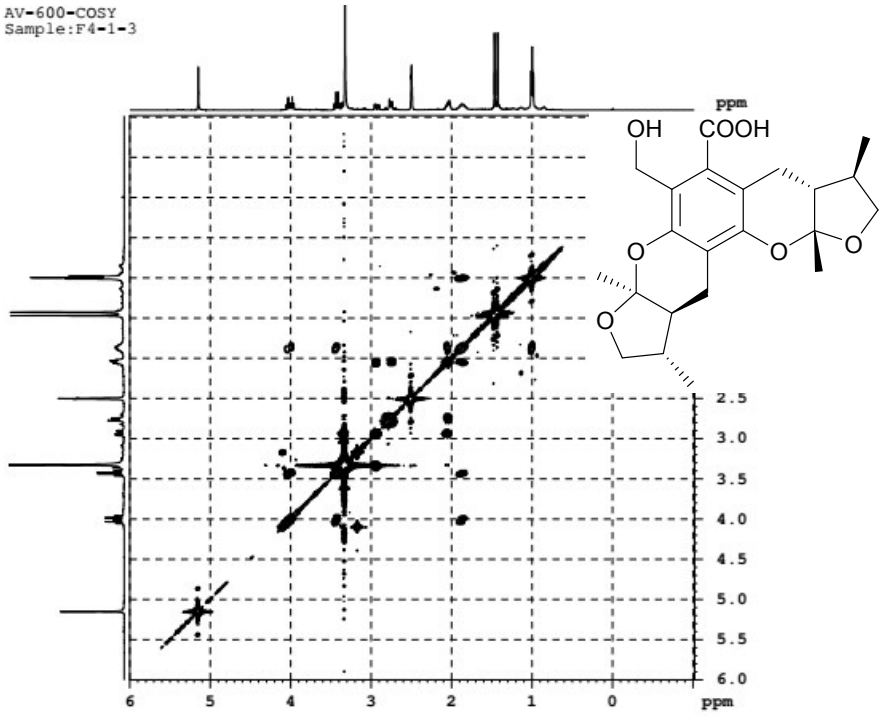

Figure S65. The DEPT-135 spectrum of compound **6**

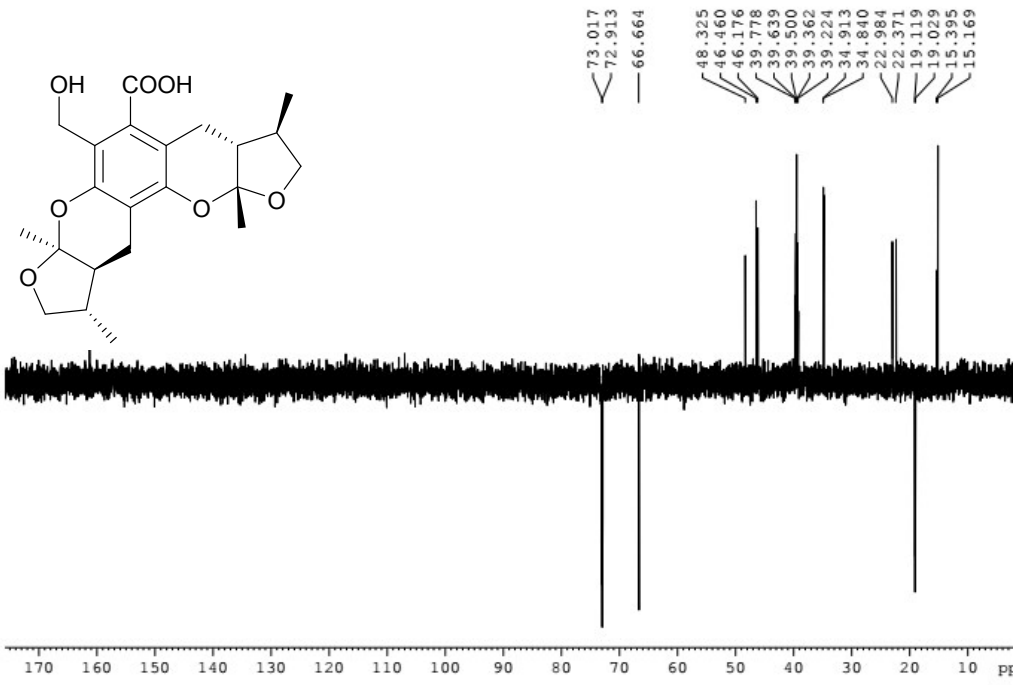

Computational details for ECD of compound **6**

Computational method

The Spartan 14.0 (Wavefunction Inc., Irvine, CA, USA) searches using molecular mechanics MMFF were performed for **6-1a**, which gave 45 conformers. The only low-energy conformer of **6-1a** accounting for more than 15% Boltzmann distribution was further optimized and analysed frequency in Gaussian 09 program package, using the density functional theory (DFT) at the B3LYP/6-31G (d, p) level and the same way in the methanol, resulted in no imaginary frequencies. Solvent effects were taken into consideration by using the conductor polarizable continuum model (CPCM). The conformer of **6-1a** was calculated electronic circular dichroism (ECD) by the time-dependent density functional theory (TD-DFT) method at the B3LYP/6-31G (d, p) level with the CPCM model in methanol solution. The calculated ECD curve of the **6-1a** was generated using SpecDis 1.51 with σ = 0.16 eV at 0 nm shift.

Table S16 Energy analysis of **6-1a**

Label	MMFF	
	rel. E(Kal/mol)	Boltzmann Dist.
6-1a	0.00	0.178

Table S17 Computational methods for ECD of **6-1a**

Standard orientation:

Center Number	Atomic Number	Atomic Type	Coordinates (Angstroms) X	Y	Z
1	6	0	-0.890803	1.918290	0.132182
2	6	0	-1.443576	0.628575	0.268248
3	6	0	-0.678289	-0.536835	0.153378
4	6	0	0.688145	-0.377756	-0.111011
5	6	0	1.287042	0.871358	-0.298051
6	6	0	0.483627	2.019051	-0.157630
7	8	0	1.461308	-1.505277	-0.250510
8	6	0	2.751368	-1.501769	0.458343
9	6	0	3.531578	-0.172601	0.218703
10	6	0	2.750550	0.830320	-0.658214

11	8	0	3.503962	-2.532078	-0.127905
12	6	0	4.425630	-1.963270	-1.082429
13	6	0	4.854588	-0.632478	-0.452151
14	8	0	-2.798892	0.591640	0.491073
15	6	0	-3.465173	-0.653890	0.910577
16	6	0	-2.828217	-1.857156	0.207693
17	6	0	-1.302392	-1.899532	0.319867
18	8	0	-4.763390	-0.561572	0.395965
19	6	0	-4.816993	-1.161842	-0.928470
20	6	0	-3.416652	-1.734301	-1.215347
21	6	0	-1.829296	3.105071	0.249945
22	6	0	1.129813	3.355076	-0.355791
23	6	0	-3.511129	-0.673847	2.426936
24	6	0	-3.439540	-3.038391	-2.014638
25	6	0	2.482865	-1.854701	1.914240
26	6	0	6.016720	-0.795307	0.536596
27	8	0	1.741811	3.689762	-1.355856
28	8	0	0.997942	4.171759	0.712167
29	8	0	-2.873222	3.089011	-0.738375
30	1	0	3.731497	0.297689	1.186509
31	1	0	2.836352	0.524164	-1.710350
32	1	0	3.221204	1.811795	-0.585939
33	1	0	3.921815	-1.820435	-2.046933
34	1	0	5.240551	-2.679556	-1.209466
35	1	0	5.148294	0.080984	-1.230406
36	1	0	-3.244699	-2.756439	0.677784
37	1	0	-1.013725	-2.313673	1.294840
38	1	0	-0.892857	-2.590459	-0.423439
39	1	0	-5.124966	-0.398840	-1.649265
40	1	0	-5.579833	-1.947716	-0.896542
41	1	0	-2.834363	-0.989842	-1.772416
42	1	0	-2.273390	3.123503	1.254204
43	1	0	-1.300972	4.045149	0.106284
44	1	0	-4.051451	0.203782	2.791543
45	1	0	-4.020851	-1.576789	2.773609
46	1	0	-2.499849	-0.658330	2.842690
47	1	0	-3.906655	-2.889867	-2.994218
48	1	0	-2.425423	-3.413496	-2.188269
49	1	0	-4.003879	-3.814363	-1.484353
50	1	0	2.023480	-2.845120	1.973871
51	1	0	3.420218	-1.861963	2.477062
52	1	0	1.810521	-1.122696	2.370654
53	1	0	6.922275	-1.128718	0.018253
54	1	0	6.241632	0.155642	1.031220
55	1	0	5.783368	-1.531999	1.313161

56	1	0	1.431302	5.019385	0.502911
57	1	0	-3.394950	2.287842	-0.573341

Table S18 2D Structures of **6-1a**

label	structure
6-1a	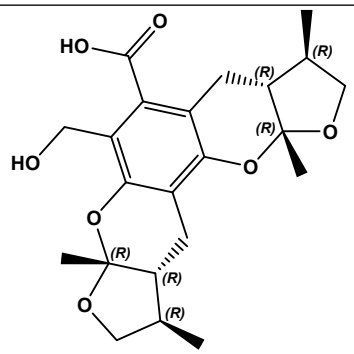
6-1b	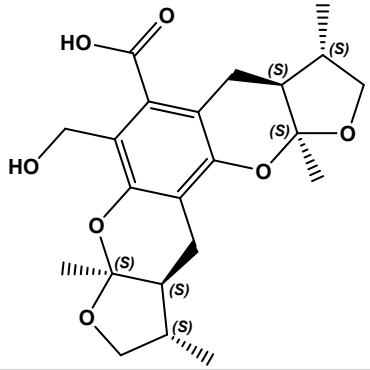

Computational methods

The Spartan 14.0 (Wavefunction Inc., Irvine, CA, USA) searches using molecular mechanics MMFF were performed for **6-2a**, which gave 48 conformers. The only low-energy conformer of **6-2a** accounting for more than 15% Boltzmann distribution was further optimized and analysed frequency in Gaussian 09 program package,[1] using the density functional theory (DFT) at the B3LYP/6-31G (d, p) level and the same way in the methanol, resulted in no imaginary frequencies. Solvent effects were taken into consideration by using the conductor polarizable continuum model (CPCM). The conformer of **6-2a** was calculated electronic circular dichroism (ECD) by the time-dependent density functional theory (TD-DFT) method at the B3LYP/6-31G (d, p) level with the CPCM model in methanol solution. The calculated ECD curve of the **6-2a** was generated using SpecDis 1.51 [2-3] with σ = 0.16 eV at 0 nm shift.

Table S19 Energy analysis of **6-2a**

Label	MMFF	
	rel. E(Kal/mol)	Boltzmann Dist.
6-2a	0.00	0.181

Table S20 Computational methods for ECD of **6-2a**

Standard orientation:

Center Number	Atomic Number	Atomic Type	Coordinates (Angstroms) X	Y	Z
1	6	0	0.692557	1.944507	0.106152
2	6	0	1.305121	0.688529	0.297177
3	6	0	0.611106	-0.512108	0.159332
4	6	0	-0.759842	-0.447997	-0.160868
5	6	0	-1.422819	0.767726	-0.372366
6	6	0	-0.668374	1.954768	-0.237672
7	8	0	-1.386795	-1.662202	-0.217673
8	6	0	-2.767094	-1.788744	-0.698198
9	6	0	-3.580457	-0.552226	-0.310004
10	6	0	-2.902501	0.762265	-0.700171
11	8	0	-3.320098	-2.845575	0.038964
12	6	0	-3.938072	-2.332865	1.251248
13	6	0	-3.829105	-0.796727	1.194714
14	8	0	2.647063	0.729139	0.588846
15	6	0	3.343956	-0.468889	1.086732
16	6	0	2.824361	-1.715442	0.364296
17	6	0	1.298523	-1.838013	0.370372
18	8	0	4.670911	-0.316365	0.668466
19	6	0	4.854195	-0.936299	-0.635291
20	6	0	3.508753	-1.582729	-1.013999
21	6	0	1.551338	3.185403	0.251624
22	6	0	-1.353770	3.274428	-0.422408
23	6	0	3.273866	-0.461014	2.602351
24	6	0	3.656607	-2.893803	-1.787735
25	6	0	-2.721166	-2.160130	-2.169101
26	6	0	-5.050706	-0.074830	1.766608
27	8	0	-1.399293	4.162058	0.413295
28	8	0	-1.928710	3.401929	-1.636212
29	8	0	2.647833	3.217302	-0.678887
30	1	0	-4.540551	-0.622404	-0.835762
31	1	0	-3.412964	1.590548	-0.197769
32	1	0	-3.045392	0.935021	-1.773714

33	1	0	-3.430834	-2.766189	2.118451
34	1	0	-4.981411	-2.667527	1.248217
35	1	0	-2.940033	-0.480021	1.753829
36	1	0	3.252519	-2.583743	0.880014
37	1	0	0.977330	-2.547723	-0.398912
38	1	0	0.966049	-2.272823	1.322450
39	1	0	5.179515	-0.171945	-1.347036
40	1	0	5.649335	-1.682834	-0.529677
41	1	0	2.932537	-0.876005	-1.623845
42	1	0	0.975519	4.089372	0.064454
43	1	0	1.939181	3.244626	1.277405
44	1	0	3.736917	0.450404	2.989641
45	1	0	2.233672	-0.494546	2.937940
46	1	0	3.801922	-1.329431	3.005346
47	1	0	4.190221	-2.733843	-2.730861
48	1	0	2.678687	-3.321480	-2.032357
49	1	0	4.215955	-3.633891	-1.203521
50	1	0	-2.167880	-3.094439	-2.296310
51	1	0	-3.735403	-2.290189	-2.556354
52	1	0	-2.220564	-1.377949	-2.746593
53	1	0	-5.195788	-0.325309	2.823087
54	1	0	-4.935057	1.012149	1.700168
55	1	0	-5.961473	-0.354744	1.224215
56	1	0	-2.375149	4.267361	-1.673053
57	1	0	3.206993	2.452410	-0.470601

Table S21 2D Structures of **6-2a**

label	structure
6-2a	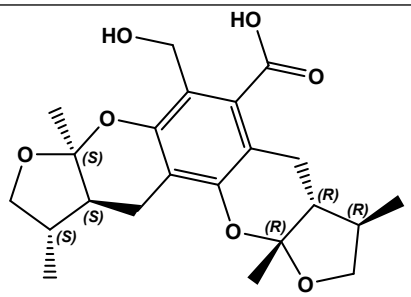
6-2b	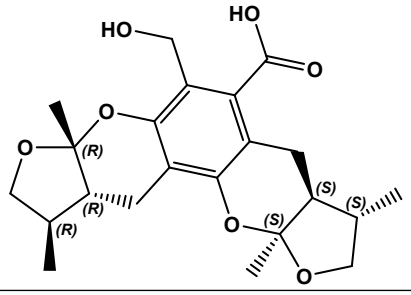

Figure S60. B3LYP/6-31 G* optimized lowest energy 3D conformer of **6-1a**

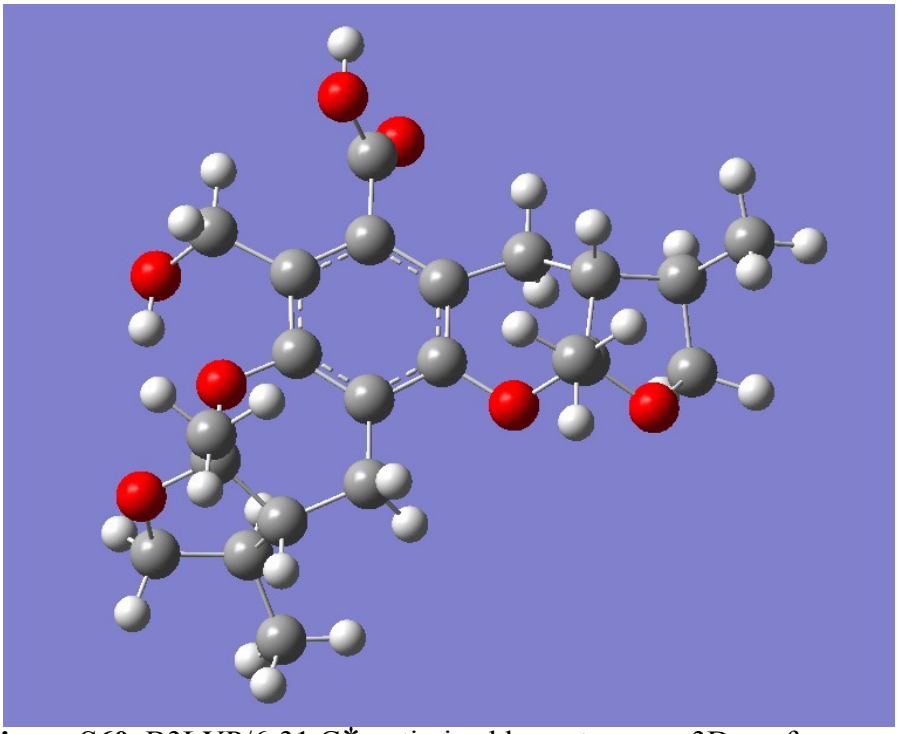

Figure S60. B3LYP/6-31 G* optimized lowest energy 3D conformer of **6-2a**

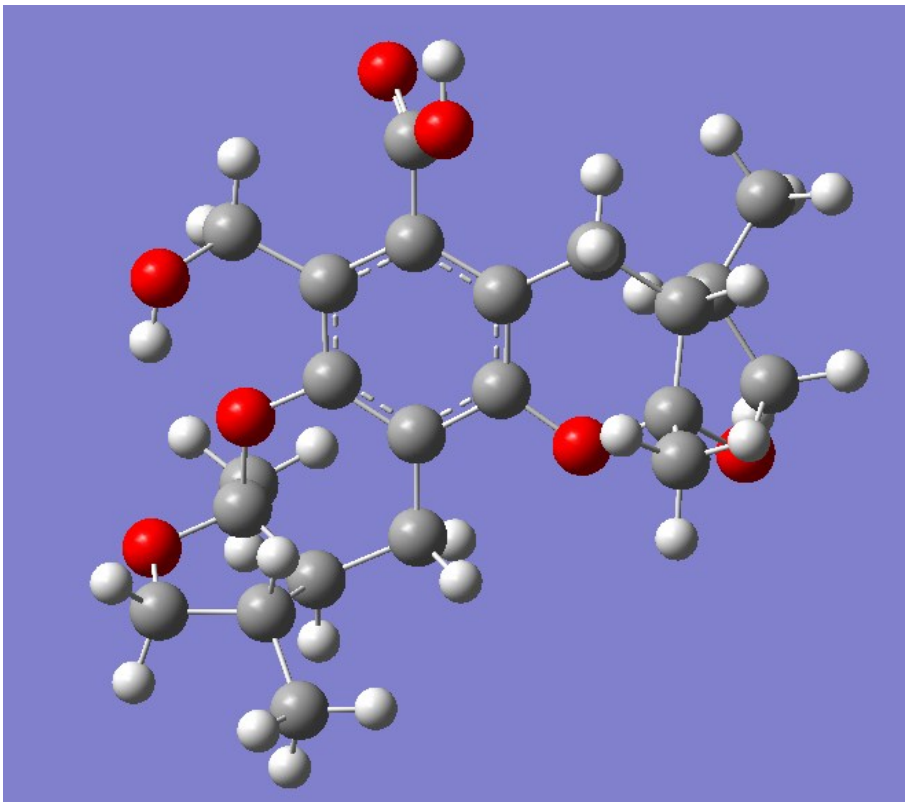

Figure S61. Experimental and suitable calculated ECD spectra of **6**